Geophys. J. R. astr. Soc. (1987) **91**, 937–983

Active tectonics of the Adriatic Region

Helen Anderson* and James Jackson *Bullard Laboratories, Madingley Rise, Madingley Road, Cambridge CB3 0EZ*

Accepted 1987 May 6. Received 1987 May 6; in original form 1986 May 28

Summary. Seismicity and fault-plane solutions show that the active deformation in the Adriatic region is very varied. West of Messina, N–S shortening occurs with slip vectors representative of the overall Africa–Eurasia motion. Along the length of peninsular Italy, NE–SW extension on normal faults is the dominant style of deformation, but changes to N–S shortening in N. Italy. Inland central and northern Yugoslavia is deforming on strike-slip and thrust faults, and an intense belt of NE–SW shortening continues south along the coast from central Yugoslavia into Albania. South of Albania the shortening in coastal regions is in a more easterly direction. The most remarkable feature of the region is the low level of seismicity in the Adriatic Sea itself, compared with the intense activity in the high topographic belts that border it on the SW, NW and NE. The relatively rigid behaviour of the Adriatic allows its motion relative to Eurasia to be described by rotation about a pole in N. Italy. Anticlockwise rotation about this pole accounts, in a general way, for the change in style and orientation of the deformation in the circum-Adriatic belts. Historical and recent seismicity account for approximately equal rates of extension in central Italy and shortening in southern Yugoslavia of about 2 mm yr^{-1}; however, these are uncertain by at least a factor of two, and are anyway likely to be underestimates of the true motion, because of the unknown contribution of aseismic creep.

The Adriatic region resembles, in some ways, other relatively stable continental blocks, such as Central Iran and the Tarim Basin, that are caught up within the distributed deformation of the Alpine–Himalayan Belt. The Adriatic, however, is bounded on three sides by the relatively stable Eurasia plate. Its boundary with the African plate is short and ill-defined by seismicity, but is likely to be located in the Southern Adriatic, near the Strait of Otranto.

The present day seismicity shows that the Adriatic, although once perhaps

* Present address: D.S.I.R. Geophysics Division, P.O. Box 1320, Wellington, New Zealand.

'a promontory of Africa', is no longer behaving in this way, and the motions on its boundaries do not directly reflect the Africa–Eurasia convergence.

Key words: seismicity, fault-plane solutions, active tectonics, Adriatic

1 Introduction

In this study we use recent and historical seismicity, fault-plane solutions, and young tectonic structures to investigate the active deformation of the Adriatic region. This study was prompted by the need to update an earlier account of the seismotectonics of the western Mediterranean (McKenzie 1972) by the addition of fifteen years of seismicity. McKenzie (1972) recognized that some features of the present deformation between the continental masses of Africa and Eurasia could be described in terms of the relative motion between several small, relatively rigid plates. He tentatively suggested that the Adriatic area is part of the African plate, but noted that there were, at that time, too few fault-plane solutions from large earthquakes to propose any tectonic interpretation with confidence. Since McKenzie's study, several earthquakes have occurred that are large enough for reliable fault-plane solutions to be determined. These new fault-plane solutions required a re-

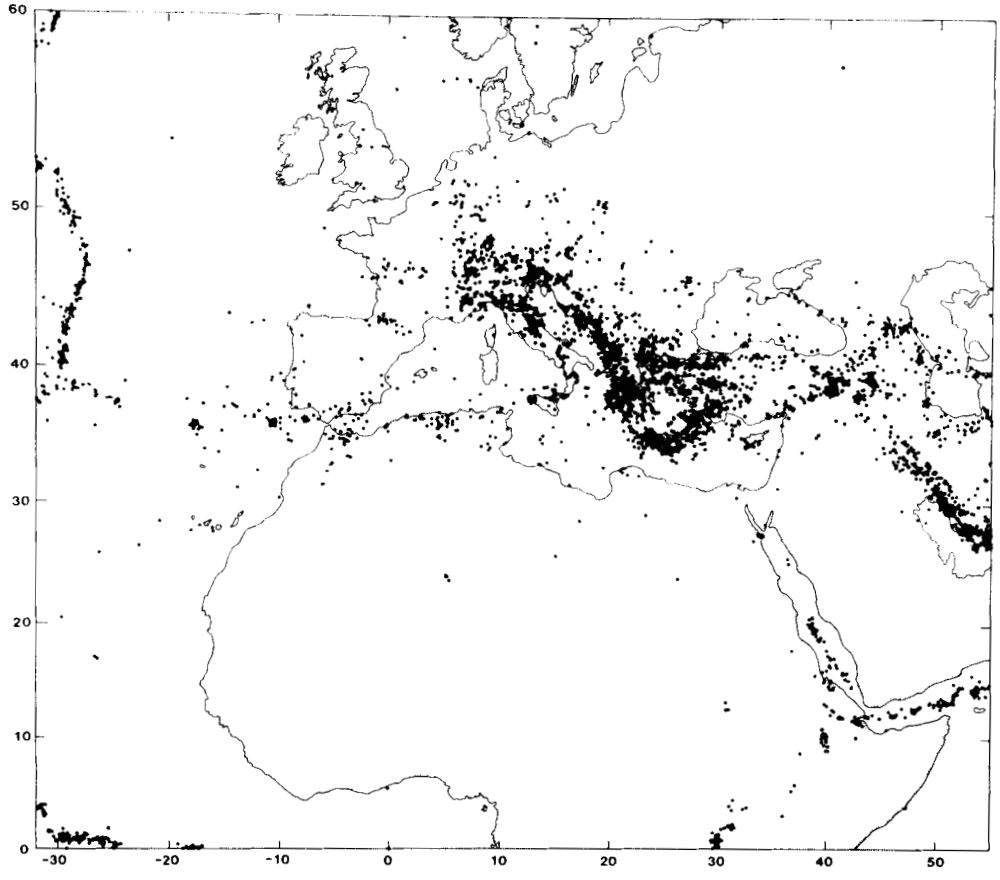

Figure 1. Seismicity of the western Alpine–Himalayan seismic belt as reported by the USGS from 1961 to 1983 August. Earthquakes with reported depths greater than 50 km are not included.

interpretation and a new kinematic description of the active deformation in the Adriatic region. This paper will not address the driving forces responsible for the observed motions.

The Adriatic region is part of the zone of distributed deformation between the African and Eurasian plates. The seismicity within this zone is diffuse (Fig. 1), but west of Sicily, the largest earthquakes occur within a somewhat narrower zone that extends through N. Africa and Gibraltar to the Azores Triple Junction. The instantaneous Africa–Eurasia pole of rotation defined by the slip vectors of these large earthquakes is located at 27.59°N, 19.74°W (Anderson 1985), which is similar to the pole positions found by Chase (1978: 29.2°N 23.5°W) and Minster & Jordan (1978: 25.2°N 21.2°W) using longer term data, including sea-floor spreading rates and transform-fault trends. Earthquake mechanisms change from normal and strike-slip faulting in the Azores region, through strike slip west of Gibraltar to thrust faulting in Sicily. This situation is summarized in Fig. 2. East of Sicily large earthquakes occur in a diffuse zone that includes Italy, Yugoslavia and Greece. Particularly intense seismicity marks the Hellenic subduction zone and the normal faulting in the Aegean Sea (McKenzie 1978).

Closer examination of the distribution of shallow earthquakes in Italy, Yugoslavia, Albania and western Greece shows that the seismicity is concentrated in land areas and that few large earthquakes occur within the area covered by the Adriatic Sea. This observation suggests that the deformation in the areas surrounding the Adriatic Sea results from the motion of this relatively aseismic, presumably relatively rigid, Adriatic block. The object of this study is to examine this seismicity in detail.

2 Promontory or microplate?

Since the first systematic geological studies of the Mediterranean, attention has been drawn to the curved nature of the mountain chain surrounding the Adriatic Sea. This chain of mountains runs through the backbone of Italy as the Apennines, curves tightly around the Po Valley as the Alps, and continues along the Yugoslavian and Albanian coasts as the Dinarides and Hellenides. In contrast with these highly deformed mountainous regions, flat areas like the Adriatic sea-floor and Apulia appear to be structurally simple. This observation led Argand (1924), among others, to suggest that the stable Adriatic area acted as a promontory of the African continent, which has been pushed into the Eurasian continent. This idea gained wide acceptance but has been challenged relatively recently by the suggestion that the stable Adriatic region is a 'microplate' or 'microcontinent' that has acted independently of continental Africa (e.g. Celet 1977).

Adria was the name first given by Suess (1883) to a previously emergent area in the position of the present Adriatic Sea. The term is used here following Channell, D'Argenio & Horvath (1979) to refer to the relatively stable Adriatic area (Po Valley, Adriatic Sea and Apulia), which is surrounded by wide mountain belts (Apennines, Alps, Dinarides, Hellenides) that mark its boundaries. Most workers appear to agree that the Jurassic and Cretaceous complexity of the Adriatic orogenic belts is best explained by a model in which Adria was then a promontory of Africa (Channell *et al.* 1979; D'Argenio, Horvath & Channell 1980; D'Argenio & Horvath 1984). That Adria continues to act as a promontory is disputed by many authors (Vandenberg & Zijderveld 1982; Celet 1977; Giese & Reutter 1978; Hsu 1982; Morelli 1984) who base their objections on interpretations of palaeomagnetism, crustal structure and recent tectonic style. These authors envisage Adria as an independent 'microplate'.

If the focal mechanisms of large earthquakes in the Adriatic area are consistent with those observed in other areas where Africa and Eurasia are in direct contact, then it is likely that

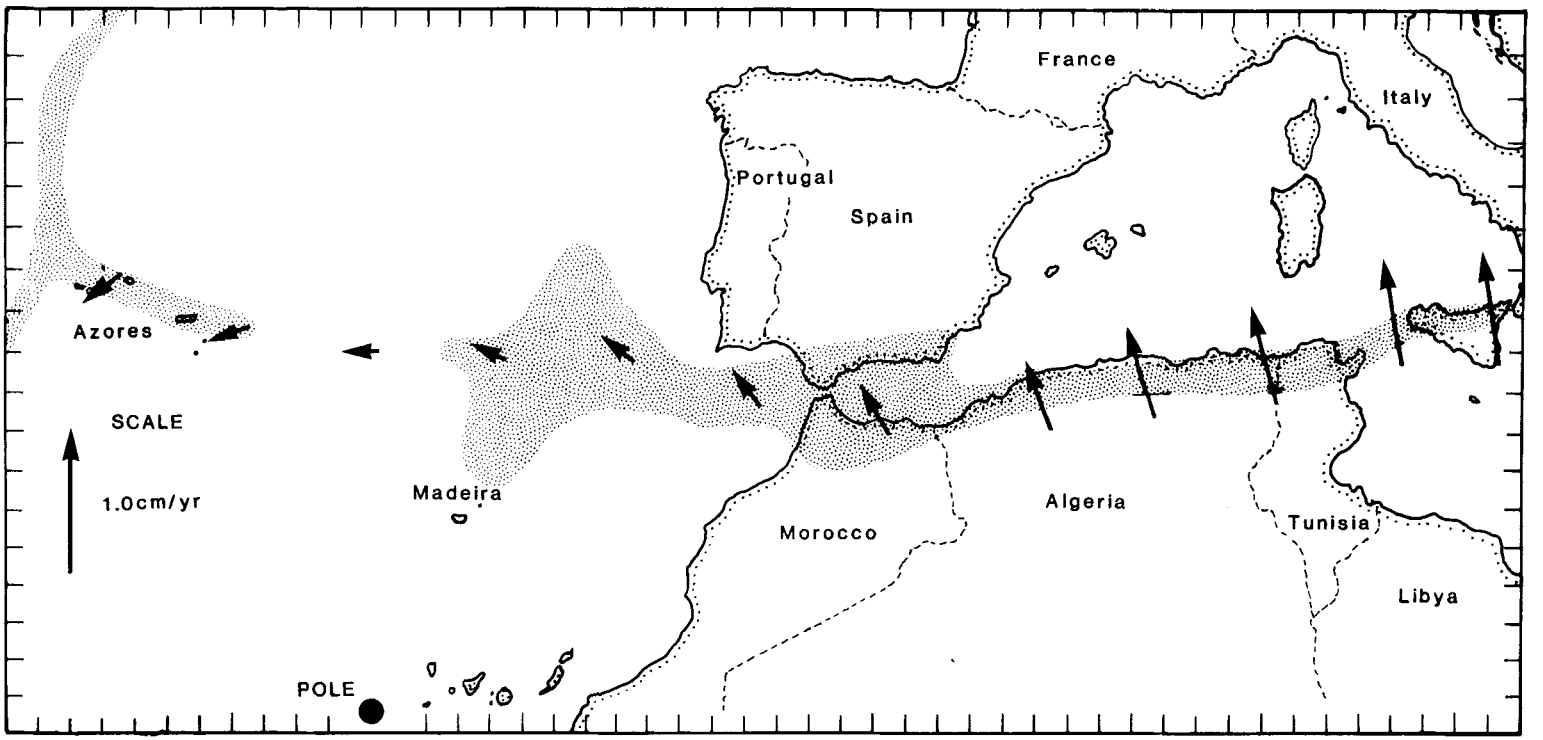

Figure 2. Slip vectors calculated for various positions along the Africa–Eurasia plate boundary. Each slip vector is calculated at the position of the centre of the arrow for an Africa–Eurasia pole of rotation located at 27.59° N, 19.74° W. The length of the arrow is proportional to the magnitude of the velocity at each point. The scale arrow is not intended to show any relative motion. Shaded areas indicate the areas of most intense seismicity.

Adria has been, and still is, a promontory of Africa. If, on the other hand, the deformation is inconsistent with the predicted overall motion between Africa and Eurasia, then Adria could be seen as an independent microplate. The seismicity cannot, however, exclude the possibility that Adria has only recently become detached from the African continent and that it acted as a promontory in the past.

Fig. 3 shows that earthquakes are concentrated in a belt that runs through the backbone

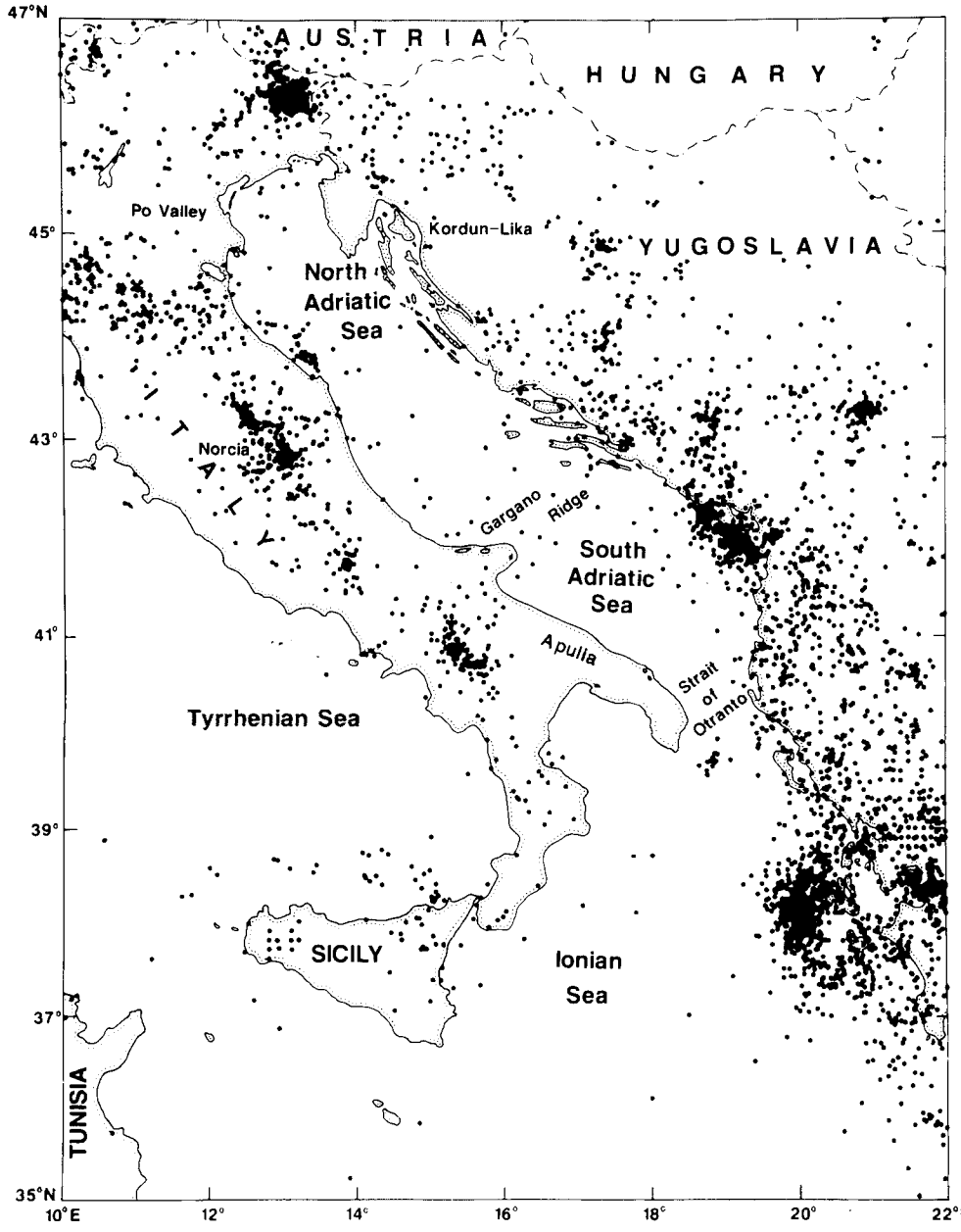

Figure 3. Seismicity of the Adriatic region, reported as shallower than 50 km by the USGS from 1963 to 1984 April. All reported events are shown, including those too small or too poorly recorded for a magnitude to be determined.

of Italy following the Apennine trend and then becomes more diffuse in the Alpine area. Intense activity marks the Albanian and southern Yugoslavian coastal regions. The Po Valley, northern and southern Adriatic basins and Apulia regions are notably less seismic. The seismicity therefore defines the wide, actively deforming margins of the Adriatic region which roughly correspond to the mountain belts where previous tectonic activity was concentrated. Although thrust faults and crustal thickening dominate the geological structure of the circum-Adriatic orogenic belts, the present-day deformation does not follow this style. Active thrusting occurs offshore along the southern Yugoslavian and Albanian

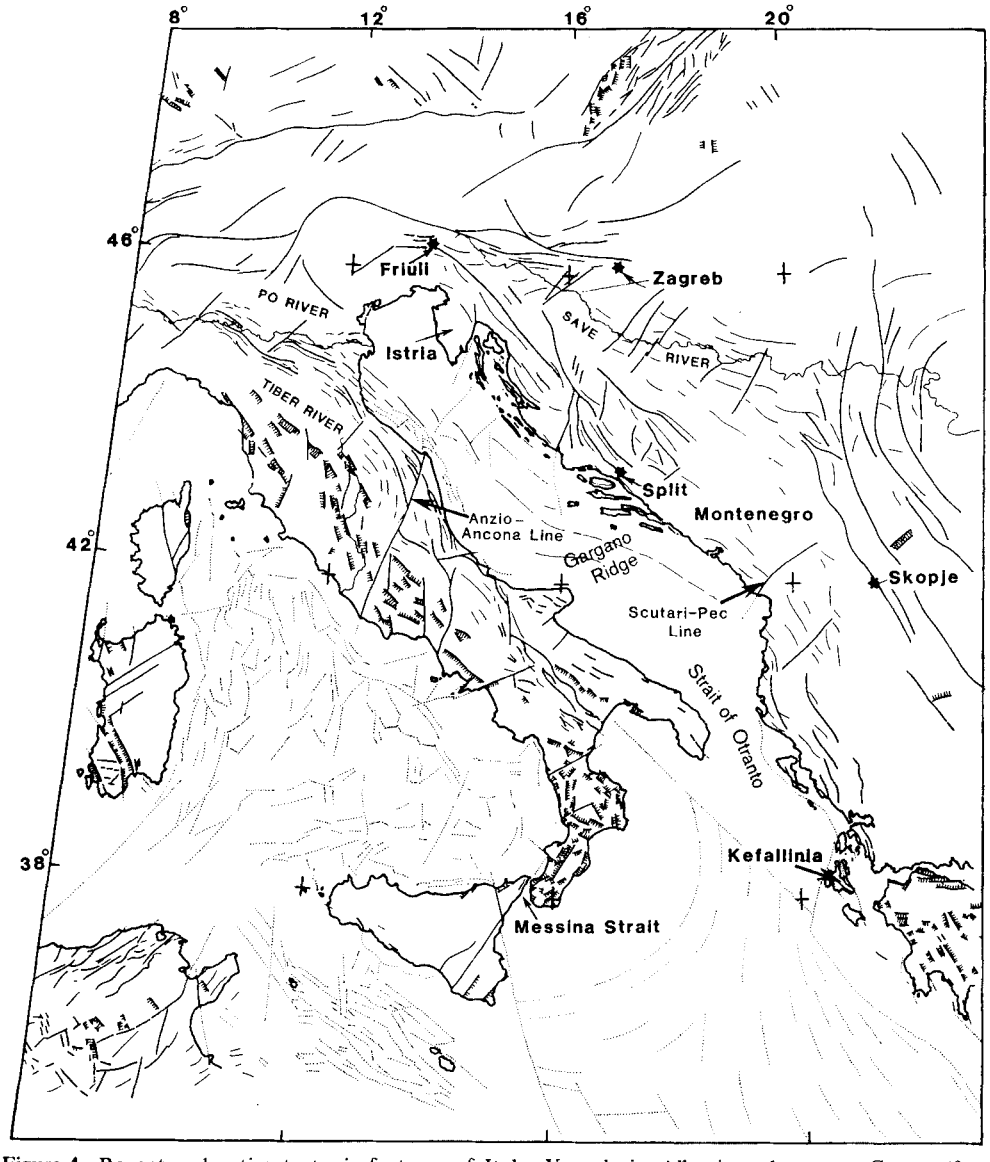

Figure 4. Recent and active tectonic features of Italy, Yugoslavia, Albania and western Greece (from Philip 1983). Heavy lines indicate a fault active in the Plio-Quaternary. Finer lines indicate axes of folds active in the Plio-Quaternary. Normal faults, such as those in central Italy, are indicated by hashing and major offshore lineaments are shown as dotted lines.

coasts (e.g. Boore *et al.* 1981) and at the northern end of the Adriatic, but normal faulting dominates the active deformation of central Italy (Fig. 4). The occurrence of active extensional tectonics in parts of the Apennines, where the older structure is dominated by major thrust sheets responsible for the crustal thickening, has confused much of the argument and literature dealing with the Adriatic.

3 Previous studies

Early authors who examined the distribution of seismicity in the Mediterranean (Barazangi & Dorman 1969; Papazachos 1973) recognized several relatively aseismic blocks. Whilst the study of seismicity patterns is useful, reliable focal mechanisms are necessary to understand the motions between such blocks. The first such comprehensive study of the Mediterranean was made by McKenzie (1972) who constructed fault plane solutions for the largest events and published the polarities used in his mechanisms so that their reliability could be assessed. Ritsema (1975) summarized the present day deformation of the western Mediterranean but offered no explanation for the motions of areas with distinctive focal mechanisms (for example, thrusting in Yugoslavia relative to normal faulting in peninsular Italy).

More recently, many poorly constrained or erroneous focal mechanisms have been published. These have usually been determined using polarity data published in agency bulletins (e.g. those of the International Seismological Centre, ISC) without examination of the relevant seismograms. Unless the polarity data can be independently checked, we do not consider such solutions to be reliable, and do not discuss them further in this study. Other studies in which mechanisms are presented without any polarity information are also not discussed unless such data are retrievable from other sources.

The inversion of long-period body waves for the centroid-moment tensor (Dziewonski, Chou & Woodhouse 1981, section 4.2) has been widely used to obtain focal mechanisms. Giardini *et al.* (1984) published centroid moment tensors for 35 moderate to large earthquakes that occurred in the Mediterranean since 1977, but did not attempt any kinematic or dynamic synthesis of the area from these data.

Our study mainly updates the work of McKenzie (1972, 1978). The additional fifteen years of data available since his 1972 study allows a much better appraisal of the seismicity in the western Mediterranean, and the use of seismic techniques developed since 1972, such as waveform modelling and relative relocation, provides a better understanding of the source geometry in large earthquakes and their aftershock sequences.

Focal mechanisms of small earthquakes, especially aftershocks, often reflect minor internal deformation of the blocks bounded by large seismogenic faults (e.g. Soufleris *et al.* 1982; Ouyed *et al.* 1983; Deschamps & King 1984; King *et al.* 1985; Westaway & Jackson 1987). Inclusion of such mechanisms in a regional study only confuses the pattern of the larger scale deformation. For this reason, only earthquakes with body-wave magnitudes greater than about 5.2 have been considered in this study. Our objective is not to look at the details of each earthquake, but rather to see how the faulting in large earthquakes is related to the regional deformation.

4 Data reduction

Focal mechanisms for 51 earthquakes, including 45 new or revised first motion fault plane solutions determined by the authors, are presented in this study (Fig. 5). Solutions for earthquakes that occurred before 1963 are mainly from McKenzie (1972), and published centroid-moment tensor solutions for events occurring in 1983 and 1984 are also included.

Table 1 lists the events, as well as an index to the figures showing their first motion polarities. The locations of these earthquakes are listed in Appendix 1 and details of their nodal plane orientations are included in Appendix 2. For convenience, all earthquakes for which a fault-plane solution is shown are identified by number or date, as in Table 1.

4.1 LOCATIONS

4.1.1 Epicentres

Most of the epicentral locations used here are those reported by the International Seismological Centre (ISC) and by the National Earthquake Information Service (NEIS) of the

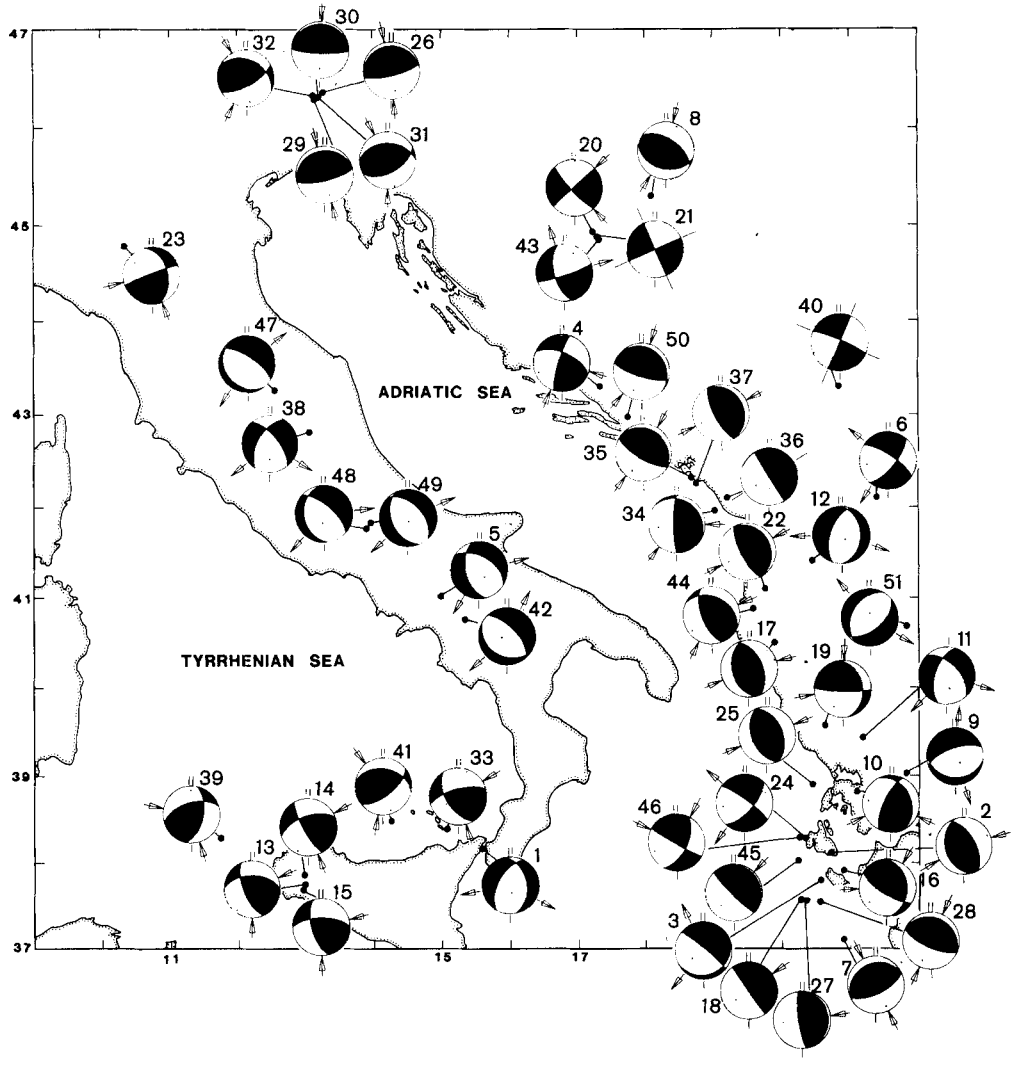

Figure 5. Fault-plane solutions for shallow earthquakes of the peri-Adriatic. Compressional quadrants are shaded and each event is numbered as in Table 1. *P*-axes are shown as a dot in the dilatational quadrant and the horizontal projections of slip vectors are shown as arrows. Location and nodal plane information is given in Appendices 1 and 2.

Table 1. Earthquakes with mechanisms shown and discussed in this study. For hypocentral locations see Appendix 1.

No.	Date	Time	m_b	M_o	M_o SF	M_o Source	Fig.	Polarity source	Text	Area	Source Vel.
1	081228	0420	7.0	-	-	-	5	-	5.7	Sicily	-
2	530812	0923	7.2	-	-	-	5	1	5.6	W.Greece	M
3	591115	1708	6.6	-	-	-	5	1	5.6	W.Greece	M
4	620111	0505	5.7	-	-	-	5	1	5.4	Yugoslavia	M
5	620821	1819	-	-	-	-	11	-	5.2	Italy	C
6	630726	0417	5.5	-	-	-	13	-	5.4	Yugoslavia	C
7	631216	1347	5.6	-	-	-	17	-	5.6	W.Greece	C
8	640413	0830	5.4	-	-	-	13	-	5.4	Yugoslavia	C
9	660205	0201	5.6	-	-	-	14	-	5.5	W.Greece	C
10	661029	0239	5.7	-	-	-	14	-	5.5	W.Greece	C
11	670501	0709	5.6	-	-	-	14	-	5.5	W.Greece	C
12	671130	0725	6.0	-	-	-	14	-	5.5	Albania	C
13	680115	0201	5.4	-	-	-	7	-	5.1	Sicily	C
14	680116	1642	5.1	-	-	-	7	-	5.1	Sicily	C
15	680125	0956	5.1	-	-	-	7	-	5.1	Sicily	C
16	680528	0739	5.4	-	-	-	17	-	5.6	W.Greece	C
17	690403	2212	5.1	-	-	-	14	-	5.5	Albania	C
18	690708	0809	5.4	-	-	-	17	-	5.6	W.Greece	C
19	691013	0102	5.6	-	-	-	14	-	5.5	W.Greece	C
20	691026	1536	5.3	-	-	-	13	-	5.4	Yugoslavia	C
21	691027	0810	5.3	-	-	-	13	-	5.4	Yugoslavia	C
22	700819	0201	5.2	-	-	-	14	-	5.5	Albania	C
23	710715	0133	5.2	-	-	-	11	-	5.2	Italy	C
24	720917	1407	5.6	-	-	-	17	-	5.6	W.Greece	C
25	731104	1552	5.8	-	-	-	14	-	5.5	W.Greece	C
26	760506	2000	6.0	-	-	-	12	-	5.3	N.Italy	C
27	760511	1659	5.8	-	-	-	17	-	5.6	W.Greece	C
28	760612	0059	5.5	-	-	-	17	-	5.6	W.Greece	C
29	760911	1631	5.2	-	-	-	12	-	5.3	N.Italy	C
30	760911	1635	5.3	-	-	-	12	-	5.3	N.Italy	C
31	760915	0315	5.7	-	-	-	12	-	5.3	N.Italy	C
32	760915	0921	5.4	-	-	-	12	-	5.3	N.Italy	C
33	780415	2333	5.5	1.39	18	1	7	-	5.1	Sicily	M
34	790409	0210	5.3	-	-	-	13	-	5.4	Yugoslavia	C
35	790415	0619	6.2	3.11	19	1	13	-	5.4	Yugoslavia	C
36	790415	1443	5.7	6.04	17	1	5	2	5.4	Yugoslavia	-
37	790524	1723	5.8	2.24	18	1	13	-	5.4	Yugoslavia	C
38	790919	2135	5.9	6.92	17	1	11	-	5.2	Italy	C
39	791208	0406	5.4	-	-	-	7	-	5.1	Sicily	C
40	800518	2002	5.7	8.85	17	1	13	-	5.4	Yugoslavia	C
41	800528	1951	5.7	3.84	17	1	7	-	5.1	Sicily	C
42	801123	1834	6.0	2.43	19	1	11	-	5.2	Italy	C
43	810813	0258	5.4	3.90	17	1	13	-	5.4	Yugoslavia	C
44	821116	2341	5.6	3.20	17	1	5	2	5.5	Albania	-
45	830117	1241	6.1	2.35	19	1	17	-	5.6	W.Greece	C
46	830323	2351	5.8	2.23	18	1	17	-	5.6	W.Greece	C
47	840429	0503	5.2	3.4	17	6	5	2	5.2	Italy	-
48	840507	1749	5.5	7.8	17	6	5	2	5.2	Italy	-
49	840511	1041	5.2	2.0	17	6	5	2	5.2	Italy	-
50	840513	1245	5.1	1.7	17	6	5	2	5.4	Yugoslavia	-
51	840709	1857	5.1	7.6	16	7	5	2	5.5	Greece	-

Notes Date given as year, month, day
Time given as hour, minute
m_b: derived from USGS listing
M_o: seismic moment
M_o SF: scale factor (10^{SF} Nm)
M_o source: 1 Giardini et al. (1985)
6 Dziewonski et al. (1985)
7 Irby et al. (1985b)

Fig. indicates figure where polarity observations are shown. If no polarities are presented, figure refers to that showing only a shaded quadrants fault plane solution but polarity source column indicates reference to available polarity information.

Polarity source: 1 McKenzie (1972)
2 No polarities, centroid-moment tensor solution only available.
Rest: this study.

Text: indicates section in the text where the event is discussed.
Source vel.: C velocity at focus 6.8 km/s
M velocity at focus dependent on depth of event but originates in the mantle.

United States Geological Survey (here referred to as USGS). Earthquake locations determined by the ISC are based on many more arrival times than those of the USGS and are probably more accurate. Some reliable macroseismic locations are available and, where used, are discussed in the text.

Earthquakes with reported magnitudes ≥ 5.0 are usually recorded by many stations, and Ambraseys & Melville (1982) have shown that large events ($m_b \geq 5.5$) in Iran are generally located within 20 km of their macroseismic epicentres. A similar accuracy is reported for earthquakes in Italy (Westaway & Jackson 1987), Algeria (Yielding *et al.* 1981), and Greece (Soufleris & Stewart 1981; Jackson *et al.* 1982a).

Relative relocation techniques can improve the accuracy of epicentral locations if the location of a reference event is known reliably, from either macroseismic evidence (damage distribution or recognition of a fault break) or a temporary local network. The relative relocation technique of Jackson & Fitch (1979) has successfully refined the locations of aftershocks in Greece and Algeria (Jackson *et al.* 1982a; Yielding *et al.* 1981) and is used here to improve the locations of a swarm of earthquakes that occurred in 1969 January in western Sicily. In this case, the location of the master shock was estimated from the maximum epicentral intensity distribution, which is quite localized for an earthquake of this relatively small magnitude ($m_b = 5.1$). This relocation method does not reliably determine focal depth because of the trade-off between depth and origin time (Jackson & Fitch 1979).

4.1.2 Focal depths

Errors in focal depths determined from arrival times are usually greater than those in epicentral co-ordinates. Reliable focal depths can be determined if the surface reflections *pP* or *sP* can be recognized in the seismogram; but these are rarely evident for earthquakes shallower than 70 km.

The depths of shallow earthquakes can be obtained using either local seismograph networks or synthetic waveform modelling. Local networks have been used successfully to determine aftershock depths in Italy and Algeria (Ouyed *et al.* 1983; Deschamps & King 1984) but such networks were generally not installed after the other large earthquakes considered in this study. In the last ten years the use of synthetic seismograms, pioneered by Langston & Helmberger (1975), has become a standard technique for refining source mechanisms and focal depths. At moderate teleseismic distances and long periods, the early part of a seismogram generally consists of direct and surface-reflected phases. The relative amplitudes of these phases are determined by the focal mechanism, and their time separation is dependent on the focal depth and velocity structure above the source. Other phases such as sea-bottom reflections and water multiples can cause additional waveform complexity. The most important parameters that affect the shape of the waveform are: (1) crustal velocity model, (2) focal mechanism, (3) source-time function, (4) depth. The crustal velocity models used in this study are mainly taken from local seismic surveys. Uncertainties in the orientation of the nodal planes in fault-plane solutions can be minimized by matching the relative amplitudes of the first two half-cycles of the waveform observed at stations of different azimuths. This method has been used to check and refine the fault-plane solutions of those earthquakes whose seismograms we modelled to obtain focal depth. The source-time function is taken to be a trapezoid with a rise, a plateau and a fall time. The time function is a major source of ambiguity for some shallow earthquakes because there is a trade-off between source-time function and focal depth (Kadinsky-Cade & Barazangi 1982; Christensen & Ruff 1985). However, the width of the first half-cycle in a waveform is

generally most sensitive to focal depth and the width of the first complete cycle is most sensitive to the total duration of the time function.

Synthetic waveforms for a range of depths are compared with the observed seismograms at various distances and azimuths and the best fit depth is adopted. The depths of large ($m_b > 5.0$) earthquakes obtained by this method are probably accurate to within 4 km (Jackson & McKenzie 1984). The scalar moment can be calculated by comparison of the observed and synthetic absolute amplitudes.

4.2 FAULT-PLANE SOLUTIONS

4.2.1 First-motion solutions

The first-motion fault-plane solutions presented in this study are based on polarities read from WWSSN seismograms. We have read all the polarities of new solutions ourselves, and critical or anomalous polarities presented by McKenzie (1972, 1978) or Jackson (1979) have been checked. Station positions on the focal sphere of events that are assumed to have occurred within the crust were calculated using a *P*-wave velocity below the source of 6.8 km s^{-1}. This approach differs from that of McKenzie (1972, 1978) who assumed a

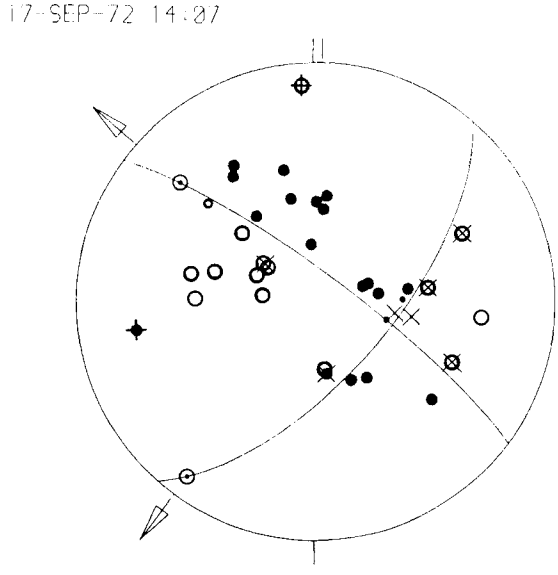

KEY:

- long period dilatation
- long period compression
- short period or uncertain dilatation
- short period or uncertain compression
- nodal dilatation
- nodal compression
- nodal (polarity uncertain)
- P axis
- T axis
- slip vector
- horizontal projection of slip vector

Figure 6. Fault-plane solution for the earthquake of 1972 September 17 (event no. 24), at 14 hr 07 min (GMT), to show the symbols and conventions used in Figs 7, 9, 10, 11, 12, 13, 14, 15 and 17. Appendices 1 and 2 give details of location and timing of each earthquake, and specifications of the nodal planes.

mantle velocity below the source of most earthquakes in this region. We therefore replotted McKenzie's fault plane solutions using focal spheres calculated with crustal source velocities. Thus the mechanisms shown here as McKenzie's (1972) may be slightly different from those he presented even though they are based on the same polarity information.

Although long-period vertical WWSSN seismograms were used for almost all polarity observations, some polarities were read on short-period vertical instruments when long-period records were unavailable or obscured. The short-period polarity observations were only used if the onset resembled the impulse response of the instrument. The long-period polarity observations were discarded if their arrival times were later than those observed on the short-period records. In cases where the polarities were critical to the nodal plane orientations, they were checked on the long-period horizontal components. It was frequently observed that the stations BUL and SHI had reversed instrumental polarities.

All the fault-plane solutions in this study are equal area, lower focal-hemisphere projections, using symbols that are shown in Fig. 6, which serves as a key for the later figures. In cases where two or more mechanisms have been determined for the same earthquake, the solution with solid nodal planes is the one we prefer. Alternative solutions are shown with dashed nodal planes and are discussed in the text.

The orthogonality of nodal planes that were determined graphically were checked using a computer program written by R. Westaway. Some of the solutions shown by McKenzie (1972, 1978) and Jackson (1979) have been adjusted accordingly, and the nodal planes listed here (Appendix 2) are therefore slightly different from those quoted in these earlier papers.

Where only one nodal plane is well constrained (the second is usually shallow dipping in this case), the focal mechanism is shown as pure dip-slip. This is not intended to imply that no strike-slip component is involved, but no better alternative can be provided without further evidence (from *S*-waves, waveform modelling, fault-break mapping, etc.). The constraints on the nodal planes are best assessed by examining the distribution of the polarity observations themselves.

4.2.2 Centroid-moment tensor solutions

Some 'best double couple' centroid-moment tensors (Dziewonski *et al.* 1981) obtained from inversion of long-period body waves are available for some of the more recent events. Where both centroid-moment tensor and first motion solutions are available for the same earthquake, the difference between them is discussed. For recent (1983–1984) earthquakes only the centroid-moment tensor solutions are available. In general, the centroid-moment tensor solutions are in reasonable, though rarely perfect, agreement with first-motion polarities. In the absence of first-motion data, the centroid-moment tensor solutions must be interpreted with care, because of their inability to resolve M_{xz} and M_{yz} components of the moment tensor for shallow events (see Scott & Kanamori 1985) and also because multiple events involving rupture on fault planes of differing orientation can lead to an 'overall' moment tensor that cannot be directly compared with particular faults (see Berberian *et al.* 1984).

5 Fault plane solutions

A large number of papers have been published on the focal mechanisms of several recent destructive earthquakes occurring in the Adriatic region (Skopje, 1963 July 26; Friuli, 1976 May 6; Montenegro, 1979 April 15; Campania-Basilicata, 1980 November 23) but no study has been made of the relationship between these and other earthquakes, less signifi-

cant in human terms, for which focal mechanisms based on teleseismic first motions can be determined. Although there are several studies of the focal mechanisms of Italian earthquakes, these either use only polarity observations from local networks (for small earthquakes), or use polarities from ISC bulletins, which we do not consider to be reliable.

Fig. 5 shows the fault plane solutions that we consider reliable for large earthquakes in the Adriatic. Appendices 1 and 2 contain details of the locations and focal mechanisms. Lists of polarities are available from the authors.

5.1 SICILY

The belt of seismicity and the main structural trends that occur along the north coast of Africa extend across the Strait of Sicily into the southern Tyrrhenian continental margin and Sicily itself. Fault-plane solutions for six earthquakes in Sicily are shown in Fig. 7. These events are shown in their regional context in Fig. 5.

The most westerly event (no. 39, 1979 December 8) has a reasonably well-constrained focal mechanism, and if the N–S trending nodal plane is chosen as the fault plane then the slip vector shows general agreement with other solutions from this area.

Further to the east, three earthquakes (nos 13–15, 1968 January 15, 16, 25) are clustered in western Sicily. The earthquake swarm including these events was studied by de Panfilis & Marcelli (1968) and Cosentino & Mulone (1985) who report maximum damage near the town of Gibellina and the Belice River (Fig. 8), although no clear fault break was recognized. The relative locations of events nos 13–15 and five other large earthquakes that also occurred in 1968 January were determined using ISC arrival time data and the relative relocation technique mentioned earlier. The location of the reference shock (1968 January 15; 0201 hr) was chosen as 37.75°N, 12.98°E, based on the maximum epicentral intensity on the isoseismal map for this event (Barbano *et al.* 1980). Fig. 8 shows the relocated positions of these events and Table 2 lists the new locations we determined. This swarm of events appears to be aligned N–S but cannot be related to any recent faulting or major structural trend. The depths determined using this relocation technique cannot be considered reliable, but the pattern of epicentres is probably accurate to about 5 km.

The mechanisms for these events (nos 13–15) were determined by McKenzie (1972) who presented them as pure thrusts because the south-dipping plane was unconstrained. Some additional polarity observations have been made and several alternative solutions (dashed) are indicated in Fig. 7. In each case, polarity observations are satisfied by either a pure thrusting mechanism or one with a NNW striking plane that dips WSW and has a right lateral strike-slip component. The alignment of the relocated epicentres in a northerly direction suggests that the solutions with appreciable strike-slip component are preferable. If so, the slip vectors for events nos 13–15 are oriented approximately N–S.

Two other large events occurred off the northern coast of Sicily but within the area of continental shelf (no. 33, 1978 April 15; no. 41, 1980 May 28). The centroid-moment tensor solution for event no. 41 (dashed line in Fig. 7) indicates almost pure dip-slip thrusting but this solution is incompatible with several of the polarities observed to the SE. Modelling of the teleseismic *P* waves for this event (Fig. 9) indicates a simple source at a depth of 12 km. The moment calculated from this modelling is 3.5×10^{17} Nm which is almost identical to that determined from the centroid-moment tensor inversion (3.84×10^{17} Nm; Giardini *et al.* 1984).

Event no. 33 (1978 April 15) was located just south of the island of Vulcano and has been studied by del Pezzo & Martini (1982) and del Pezzo *et al.* (1984). Del Pezzo & Martini

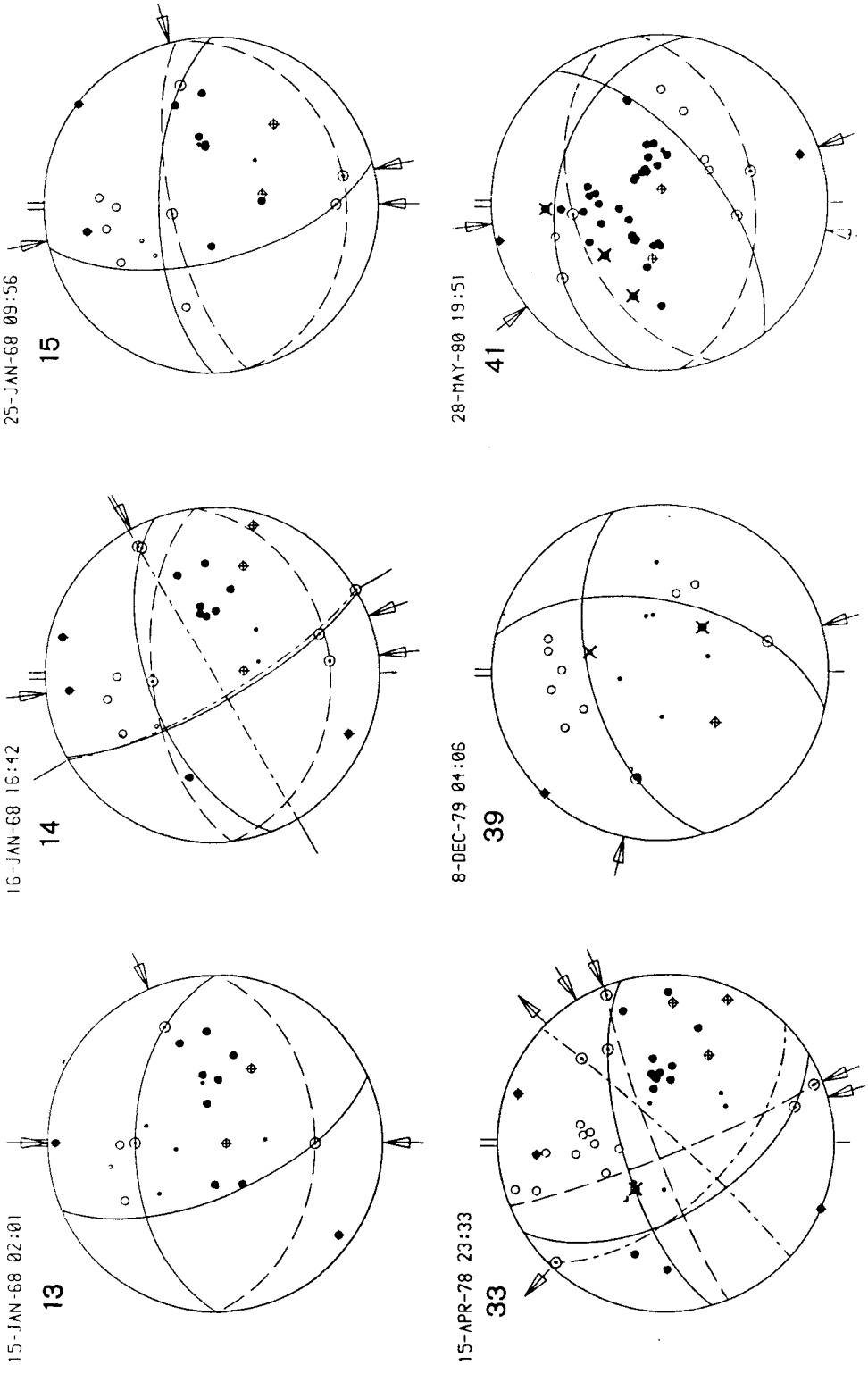

Figure 7. Focal mechanisms of shallow earthquakes in Sicily and the southern Tyrrhenian margin. Symbols as in Fig. 6.

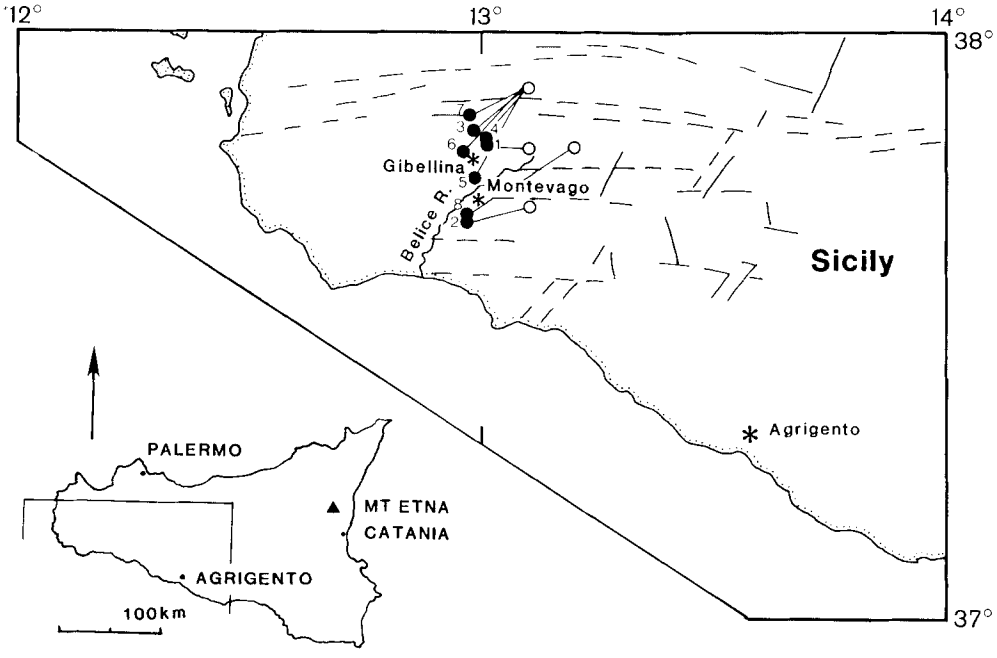

Figure 8. Relocated epicentres for the largest events in the 1968 January earthquake swarm in western Sicily. Open circles indicate ISC positions before relocation, and the number beside the filled circle identifies the event in Table 2. Thin lines show structural lineaments recognized by de Panfilis & Marcelli (1968).

(1982) relocated the aftershocks of this event, but the pattern of epicentres they obtained does not show a clear trend.

Del Pezzo *et al.* (1984) relocated epicentres for the whole Aeolian region, using two different velocity models. There is a strong gradient in crustal thickening in this area with an increase in the depth of the Moho from about 20 km in the most northern part to about 35 km under Calabria and Sicily (Morelli *et al.* 1975). The first velocity model chosen by del Pezzo *et al.* for relocation of the Aeolian earthquakes is characteristic of the northern part of the islands with a crustal thickness of 20 km. The second model places the Moho at 28.7 km ('a sort of average between two different structures'; del Pezzo *et al.* 1984). The two different velocity models lead to very different hypocentre distributions, but neither of these relocations shows any alignment of the low-magnitude seismicity with any major structural feature.

Table 2. Macroseismic location of mainshock (1968 January 15) and location of other earthquakes in W. Sicily relocated relative to this event (see Fig. 8).

Mainshock No.	Lat.	Long.	Depth (km)	Mag.	Hr	Date
1	37.807	13.012	19.0	5.1	1228.4	140168
2	37.676	12.966	1.0	5.0	1315.7	140168
3	37.830	12.983	22.0	4.7	1548.5	140168
4	37.817	13.006	34.0	5.1	133.0	150168
5	37.750	12.983	13.0	5.4	201.1	150168
6	37.793	12.960	23.0	4.6	318.7	150168
7	37.857	12.976	36.0	5.1	1642.7	160168
8	37.687	12.966	3.0	5.1	956.8	250168

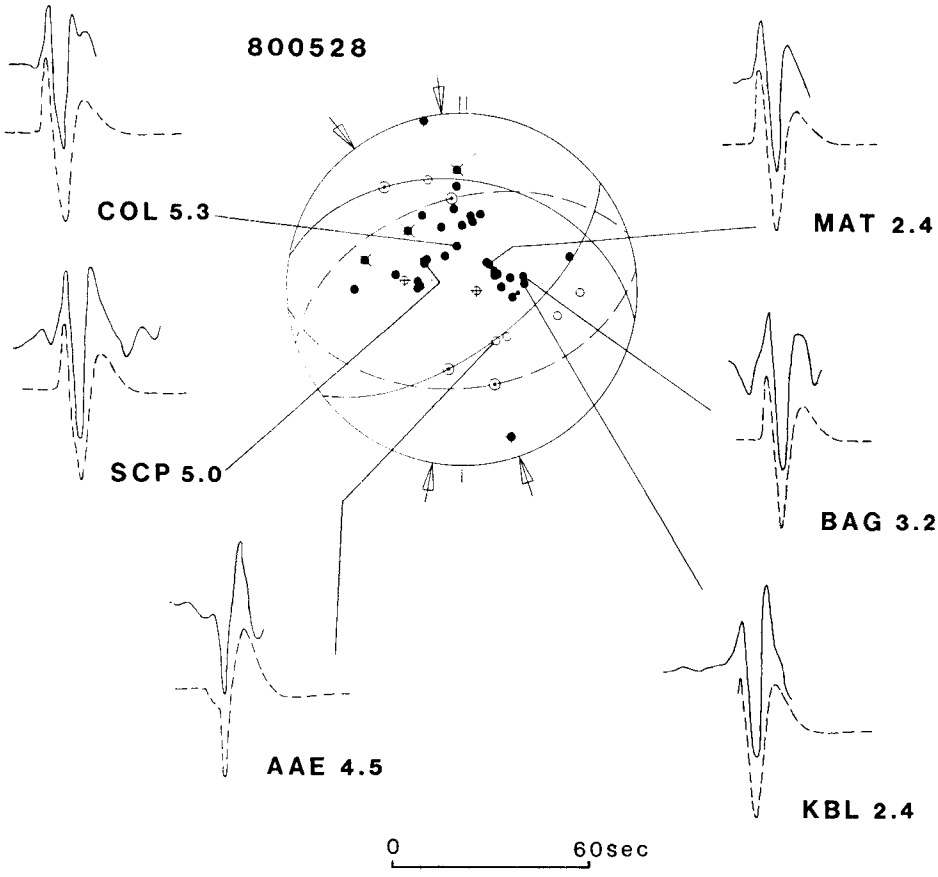

Figure 9. Observed (solid) and synthetic (dashed) waveforms for event no. 41 (1980 May 28) at a focal depth of 12 km. Synthetic waveforms were calculated using the solid nodal planes. WWSSN station code and moment ($\times 10^{17}$ Nm) are indicated by each waveform pair. A velocity model identical to that used for modelling event no. 33 (Table 3) was used, and direct waves and reflections from each interface were included. A triangular time function of 1, 0, 1 s was used.

The focal mechanism for event no. 33 (1978 April 15) was determined from first-motion data (solid and dashed lines) and the centroid-moment tensor inversion (dash and dotted line in Fig. 7; from Giardini *et al.* 1984). The nodal planes in the moment tensor solution violate two short-period compressional onsets near the null axis (Fig. 7). A third set of nodal planes, involving more strike slip motion but inconsistent with a nodal dilatational onset to the northwest, is shown by dashed lines in Fig. 7. To try and constrain this focal mechanism and determine the focal depth, we modelled the *P*-waves from this event (Fig. 10). The velocity model chosen was that determined by del Pezzo & Martini (1982) with the Moho at 20 km. The nodal planes were adjusted to fit the amplitudes of the first half cycle. The solution shown as the solid nodal planes in Fig. 7 is compatible with both these amplitudes and the polarity observations. It is clear, however, that this event did not involve a single, simple rupture. Second and third ruptures (or sub-events) with time delays of 6 and 15 s occurred, apparently to the southeast of the mainshock (see Table 3 for details). There is no independent evidence for the orientation of faulting in these second and third sub-events so their mechanisms have been assumed to be the same as that of the mainshock. The focal

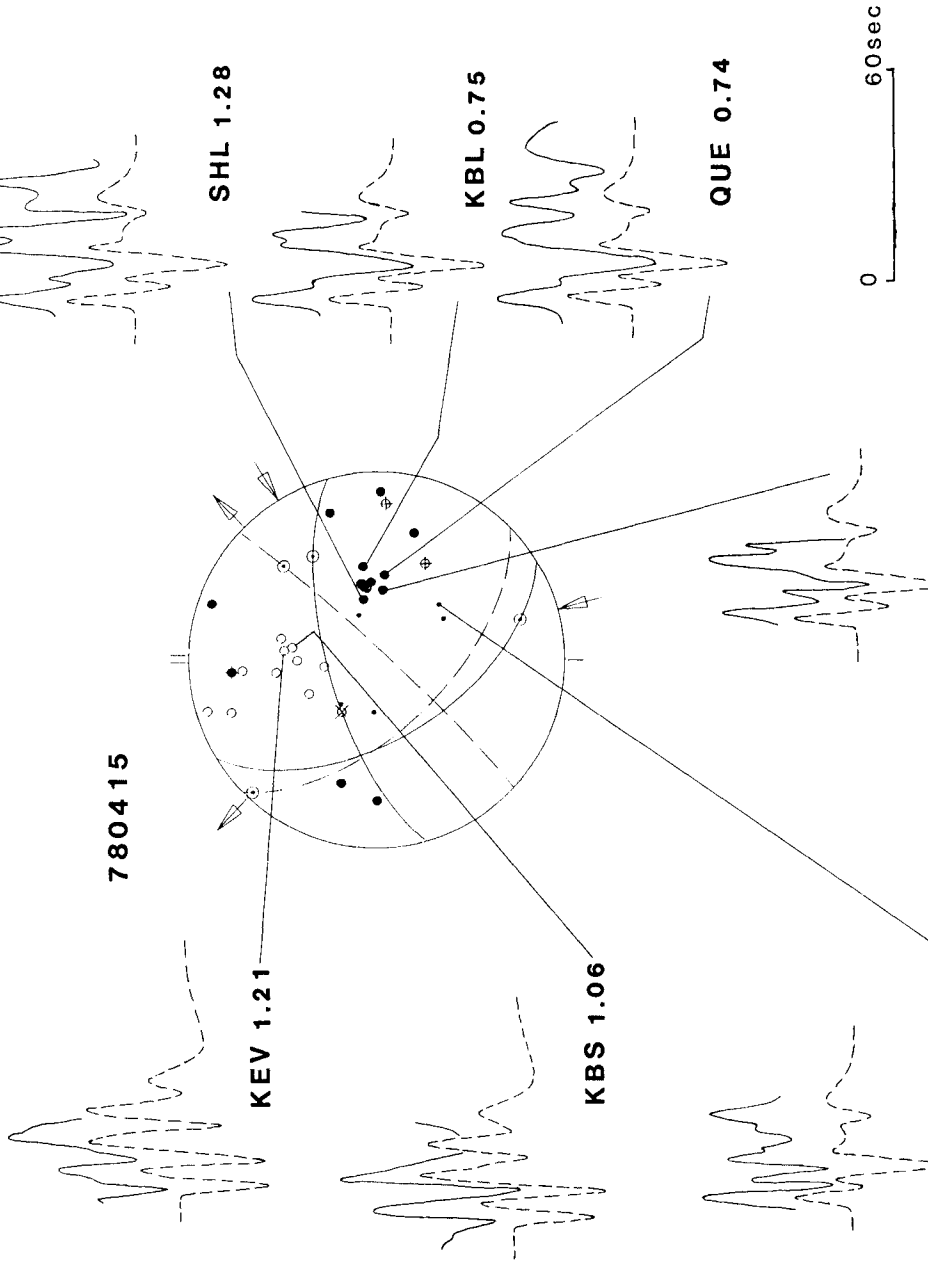

Figure 10. Observed (solid) and synthetic (dashed) waveforms for event no. 33 (1978 April 15) at a focal depth of 21 km. Synthetic waveforms were calculated for the solid nodal planes. WWSSN station code and calculated moment ($\times 10^{18}$ Nm) are shown beside each waveform pair. Details of modelling parameters are shown in Table 3.

depth of all three sub-events is estimated at about 21 km. The seismic moment of 9.7×10^{17} Nm estimated from waveform modelling is in reasonable agreement with that of 1.39×10^{18} Nm obtained by inversion for the moment tensor by Giardini *et al.* (1984). This event therefore involved complex thrust faulting which, because of the apparent rupture propagation towards the southeast, suggests that the NW-striking nodal plane may have been the fault plane. There is some independent evidence for NW-trending faulting in this area (Fig. 4 and the Tindari–Letojanni fault system of Ghisetti, Scarpa & Vezzani 1982).

Slip vectors for each of the Sicilian earthquakes discussed here appear to reflect the N–S directed convergence of Africa and Eurasia predicted in this area from the Africa–Eurasia pole of rotation (see Fig. 2).

5.2 CENTRAL ITALY

Fault-plane solutions for seven earthquakes on the Italian peninsula are shown in Fig. 5. Of these, three (nos 47–49) occurred in 1984 and insufficient seismograms were available for first-motion fault-plane solutions to be determined. The most southerly events, in the

Table 3. Model parameters used for *P*-wave modelling of event no. 33 (1978 April 15).

Subevent No.

	Strike	Dip	Rake	Moment	ΔT	ΔX	ΔY
1	148	55	154	1.0	0	0	0
2	148	55	154	1.0	6	−15	7
3	148	55	154	0.8	15	−17	15

ΔT is time delay, ΔX, ΔY are north and east offsets in km respectively. A triangular time function of 2, 0, 2 was used for all subevents.

Velocity model

Layer no.	*P*-wave km s^{-1}	*S*-wave km s^{-1}	Density Mg m^{-3}	Thickness km
1	0.001	0.001	0.001	0
2	1.5	0.001	1.0	0.7
3	4.64	2.67	2.5	4.3
4	5.68	3.27	2.8	5.0
5	6.58	3.8	2.9	10.0
6	7.85	4.53	3.3	25.0

Stations

	Distance (degrees)	Azimuth	Ray parameter
QUE	43.17	84.76	0.072
KBL	43.20	77.87	0.071
AAE	36.17	136.73	0.075
KEV	32.08	7.79	0.077
KBS	40.54	359.08	0.073
LAH	48.33	77.87	0.069
SHL	64.70	76.58	0.057

Direct waves and reflections from each interface were modelled.

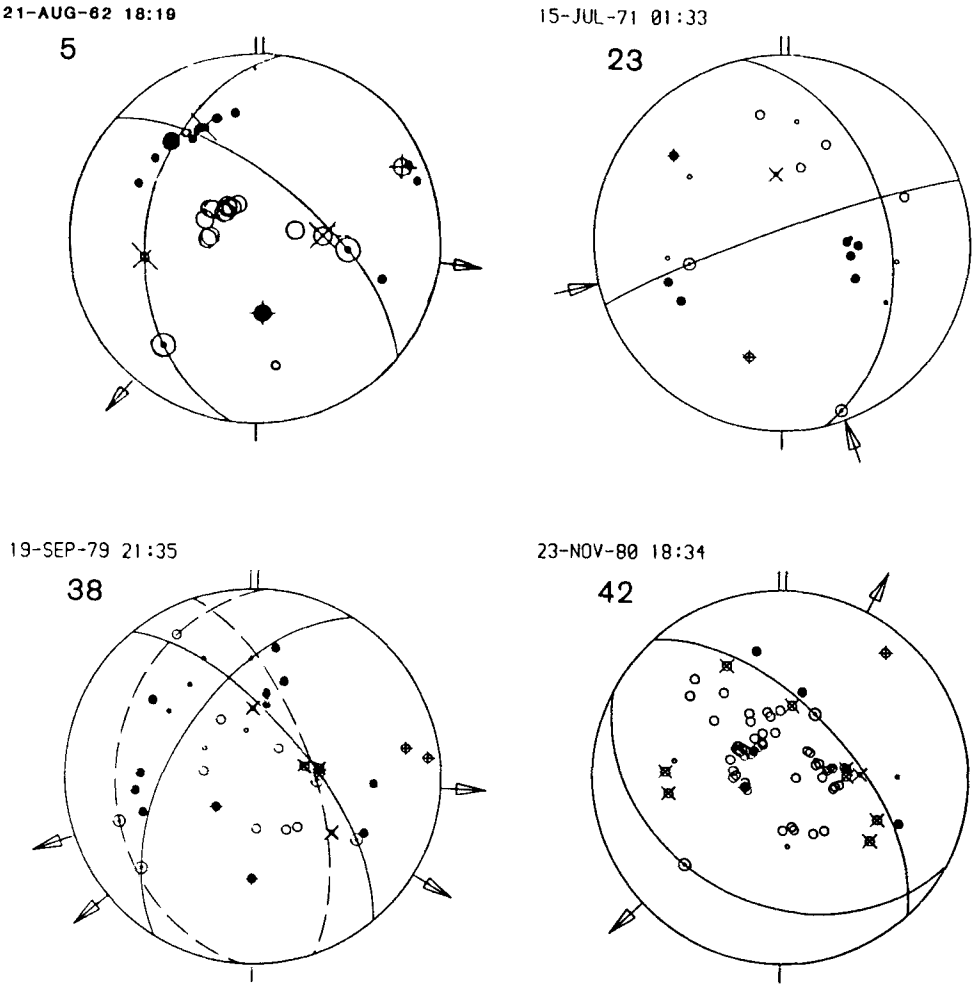

Figure 11. Fault plane solutions for peninsular Italy. The solution for event no. 5 (1962 August 21) is from Westaway (1987) and the polarities for no. 42 (1980 November 23) are from Westaway & Jackson (1987). Symbols as in Fig. 6.

Campania area, have recently been studied in detail by Westaway (1987) and Westaway & Jackson (1987). Polarities for four of the Italian events (no. 42, 1980 November 23; no. 23, 1971 July 15; no. 38, 1979 September 19; no. 5, 1962 August 21) are shown in Fig. 11.

The Campania–Basilicata earthquake (no. 42) was the largest (M_s = 6.9) to have occurred in peninsular Italy this century. The mainshock mechanism and aftershock distribution have been studied by Westaway & Jackson (1987), Deschamps & King (1983, 1984) and many others (see Westaway & Jackson 1987 for a review). Surface faulting in this earthquake shows that the NE-dipping nodal plane was the fault plane (Westaway & Jackson 1984). Aftershock studies by Deschamps & King (1983 and 1984) support this choice of fault plane. *P* and *SH* waveform modelling shows that this event was a complex multiple rupture nucleating at about 10 km depth (Westaway & Jackson 1987).

The fault-plane solution of another earthquake which occurred in the Campania region (no. 5, 1962 August 21) was published by McKenzie (1972). His first-motion polarities have

been replotted with a crustal velocity at the focus and a solution very similar to that determined by Westaway (1987; fig. 11) is shown in Fig. 5. Relocation of this event, along with local geological structure seen in seismic reflection profiles, suggest that the NE-dipping nodal plane is the fault plane, and the waveform modelling indicates that both this earthquake and its large aftershock nucleated at about 8 km depth (Westaway 1987). This modelling and the depth of 10 km determined for event no. 42 (1980.11.23) indicate that extension in the southern Apennines occurs by steep normal faulting in the upper 10–15 km of the crust.

In 1984 May, two earthquakes occurred in central Italy in the Abruzzi–Lazio area (no. 48, 1984 May 7; no. 49, 1984 May 11). The first of these was relatively large (M_s = 5.8) and caused extensive damage in the Abruzzi area. The centroid moment-tensor solutions for both these events (Dziewonski *et al.* 1985) show normal faulting with an orientation very similar to that in event no. 5 (1962.8.21). These events are located near some major N–S and NW–SE trending faults (Fig. 4), but there is no conclusive field evidence to favour either nodal plane as the fault plane. This ambiguity leads to an uncertainty in the slip vector direction of event no. 48 of about 30°. Moments of 7.82×10^{17} Nm and 2.03×10^{17} Nm were determined by Dziewonski *et al.* (1985) for events nos 48 and 49, respectively.

The Norcia, or Umbrian, earthquake 1979 September 19 (no. 38) occurred very close to the Anzio–Ancona line (Fig. 4) which trends approximately NNE and separates the northern and southern Apennines. The first-motion fault-plane solution for this event is shown in Fig. 11 along with the moment-tensor solution of Giardini *et al.* (1984), which is shown by dashed nodal planes. First motion solutions have also been determined by Deschamps, Iannaccone & Scarpa (1984), Gasparini *et al.* (1980) and Gasparini, Iannaccone & Scarpa (1985). All of these solutions show dominantly normal faulting. The first-motion solution here is well constrained, and inconsistencies of first motions with the centroid moment-tensor solution may indicate source complexity.

Deschamps *et al.* (1984) located the aftershocks of the Norcia earthquakes. They found at least two clusters of aftershock activity, which they thought revealed an elongated pattern of seismicity extending for about 8 km parallel to the Apennine trend. They then used this aftershock distribution to suggest that the nodal plane striking NW in the fault-plane solution of the mainshock was the fault plane. However, the trend in the aftershock distribution is weak and we believe that the choice of fault plane is unresolved. Although normal faulting farther south in the Campania region occurs on NW striking faults, the proximity of the Norcia earthquake to such a major structural feature as the Anzio–Ancona Line may suggest movement on a NE striking fault. Lavecchia, Minelli & Pialli (1984) report recent left lateral motion on NNE–SSW shear zones in the Umbrian area. If the NE-striking nodal plane in the fault-plane solution was the fault plane, then it too would have a component of left lateral strike-slip motion. The slip vector on the NE-striking plane is similar in direction to that in the large normal-faulting events further south. A seismic moment of 6.92×10^{17} Nm was determined by Giardini *et al.* (1984), which compares well with the value of 7.0×10^{17} Nm determined by Deschamps *et al.* (1984).

The earthquake of 1984 April 29 (no. 47), near the Tiber River, occurred in an area of NW–SE trending, recently active, grabens (Fig. 4). Only a centroid moment-tensor is available for this event (Dziewonski *et al.* 1985). It shows normal faulting with only a small component of strike-slip, so the slip vector direction is almost the same on both nodal planes. It is probable that the steeper nodal plane was the fault plane, as in the Campania area further south (Westaway 1987; Westaway & Jackson 1987).

The earthquake of 1971 July 15 (no. 23) occurred further north near the Po River. Its fault plane solution (Fig. 11) is not particularly well constrained, although a similar solution is

also reported by Gasparini *et al.* (1985). Major structural trends change from a NW–SE to an E–W trend in this area but there is no clear reason for choosing either nodal plane as the fault plane. The slip vector on the E–W nodal plane is very similar to those of the other large earthquakes in the Italian peninsula.

5.3 NORTHERN ITALY

North of the Po Valley, epicentres are not concentrated in clearly defined zones (Fig. 3), but in the last twenty years the seismicity pattern has been dominated by a swarm of earthquakes in the Friuli area (Fig. 4). Five events large enough for fault-plane solutions to be determined occurred within four months of the largest shock of this sequence (1976 May 6, no. 26).

The Friuli earthquake swarm has been the subject of many studies (e.g. Cagnetti & Pasquale 1979; special issue of *Bollettino di Geofisica*, vol. **XIX**, 72, 1976), and focal mechanisms have been presented by Cipar (1980, 1981). We collected some additional polarity observations and our solutions for these events (no. 26, 1976 May 6; nos 29–32, 1976 September 11a, b and 15a, b) are presented in Fig. 12. Our polarity observations for the mainshock (no. 26) are shown with the nodal planes determined by Cipar (1980), because the shallow dipping plane in his solution is constrained by *SH* and *SV* waveforms. Cipar (1980) calculated a focal depth of 8 ± 2 km and a seismic moment of 2.9×10^{18} Nm for the mainshock from long-period *P*-wave modelling. A similar depth of 6.5 km was estimated by Zonno & Kind (1984), using depth phases identified at regional distances by the Grafenberg array.

Four aftershocks of the Friuli earthquake (nos 29–32) were large enough for first-motion solutions to be determined. Event no. 29 is not well constrained, but observed polarities are consistent with a mechanism almost identical with that of the mainshock. The steeply dipping plane of event no. 30 is well constrained but the choice of a shallow dipping plane as the fault plane is again arbitrary. This mechanism is shown as a pure thrust, in spite of a dilatational onset at TRI, because the close proximity of this station to the epicentre (0.76°) makes its position on the focal sphere highly dependent on local velocity structure.

In contrast to the three large earlier events, first motion polarities for both the two aftershocks occurring on 1976 September 15 (nos 31, 32) require a component of strike-slip motion. Both of these mechanisms are well constrained, and Cipar (1980) determined a depth of 6 km for event no. 32.

No surface faulting was observed following any of these earthquakes, and so their correlation with specific faults has been difficult. Weber & Courtot (1978) recognized several trends of faulting, but with E–W striking thrusts the most dominant. They suggested that movement in the mainshock (no. 26) occurred on a NNE striking, left-lateral strike-slip fault. The *S*-wave data of Cipar (1980), which control the orientation of the shallow dipping nodal plane for this event, suggest that this interpretation is incorrect, and that faulting probably occurred on one of the E–W striking thrusts dipping shallowly to the north (Fig. 4), which have been recognized in this area. The northward dipping nodal planes for aftershock nos 31 and 32 are steeper than in the earlier three events, but the slip vectors on these nodal planes are all similar and are oriented approximately NNW. This slip-vector direction is in complete contrast to that observed in peninsular Italy.

5.4 YUGOSLAVIA

Recent large earthquakes have been concentrated in three main zones in Yugoslavia: the Banija area of northern central Yugoslavia (near 45°N, 17°E); the Dalmation coast south of

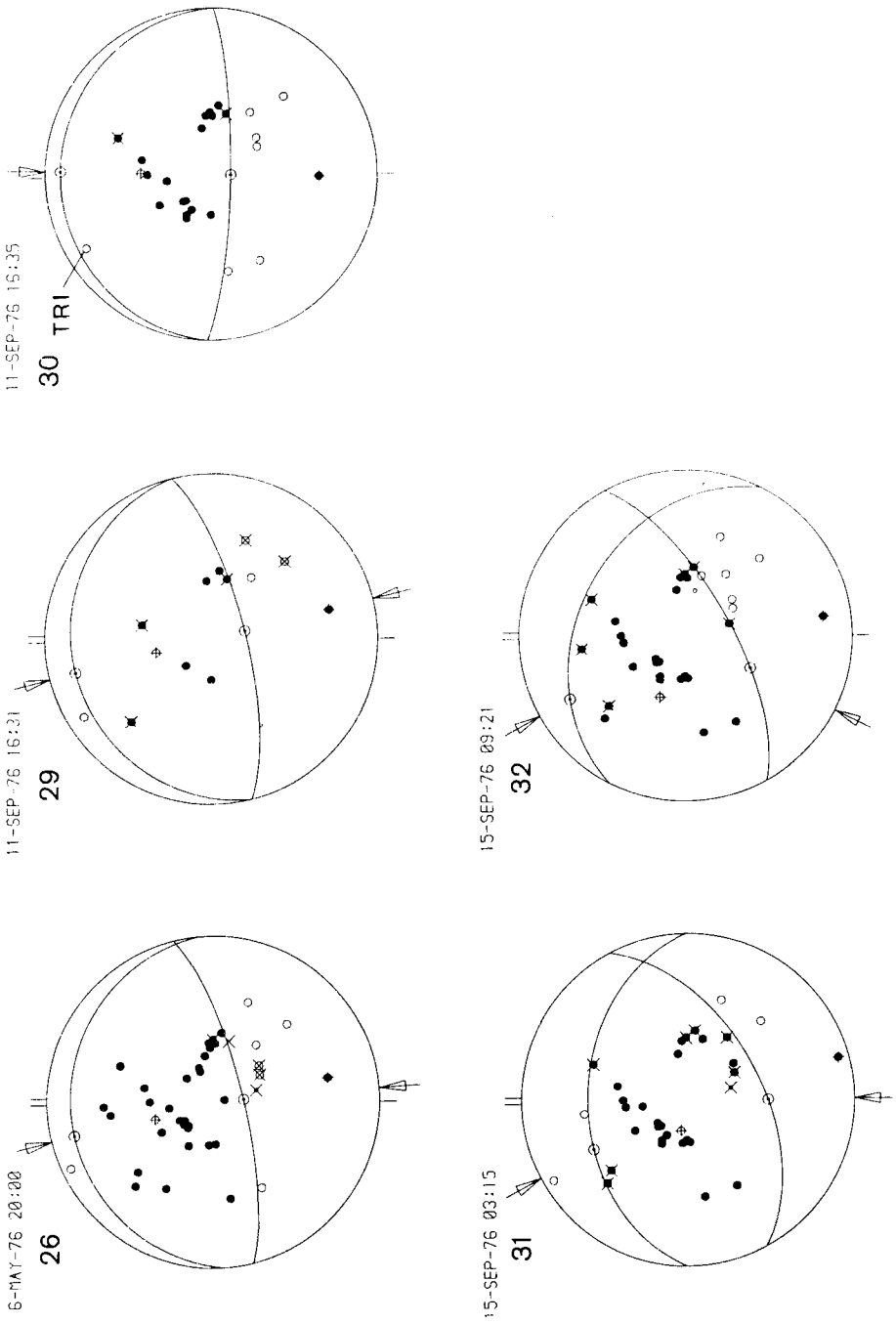

Figure 12. Fault plane solutions for the Friuli earthquakes. Symbols as in Fig. 6.

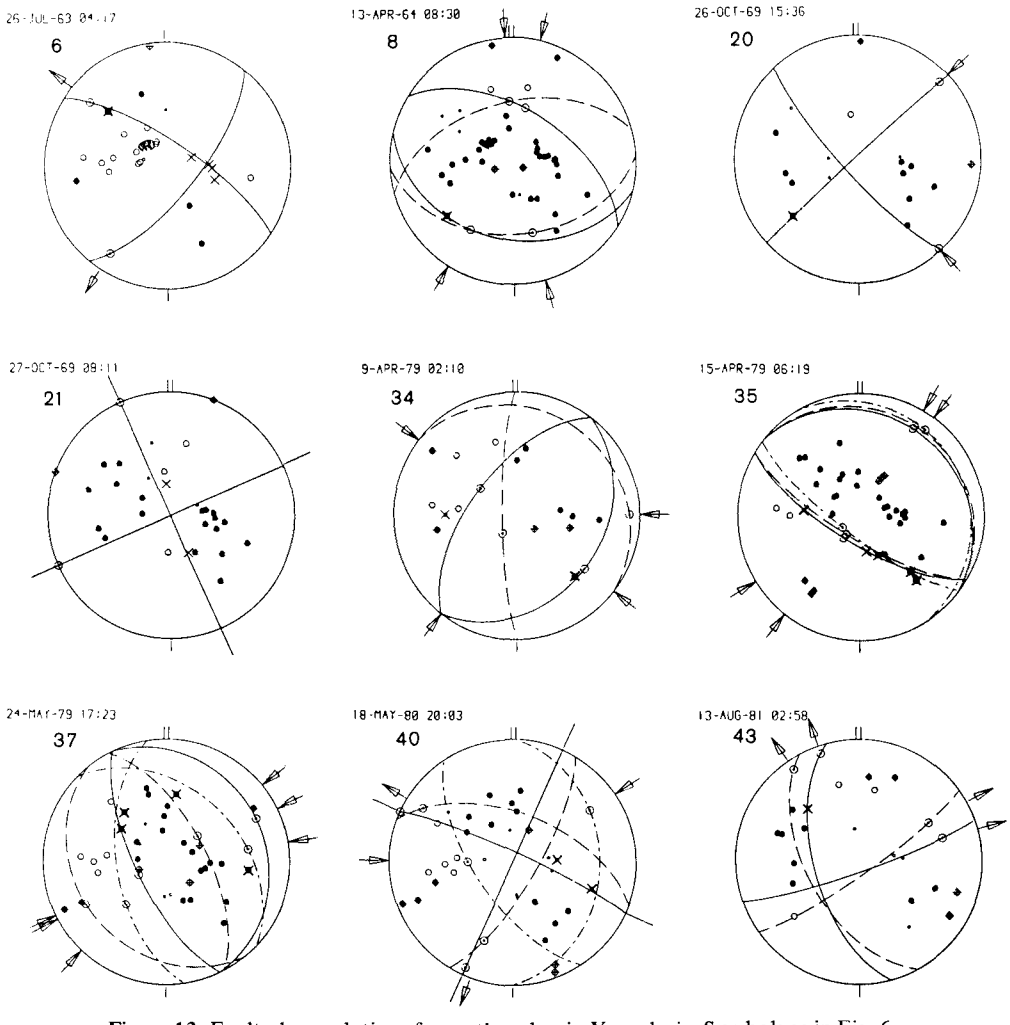

Figure 13. Fault plane solutions for earthquakes in Yugoslavia. Symbols as in Fig. 6.

Split; and an area of southern Serbia and Macedonia near Skopje (Figs 4 and 5). First-motion polarities for some of these events are shown in Fig. 13.

5.4.1 Northern central Yugoslavia

The most northerly cluster of seismicity occurs south of Zagreb near the Save River, where a set of active faults crosscuts the NW–SE structural trend of the Dinarides (fig. 4, Cvijanovic & Prelogovic 1977). There is a marked difference between the strike-slip mechanisms of three closely grouped events, no. 20 (1969 October 26), 21 (1969 October 27), and 43 (1981 August 13), and the more northeasterly thrusting mechanism of event no. 8 (1964 April 13). The first-motion solution of event no. 20 is not well constrained and polarities could also be consistent with an E–W striking thrust. However, the similarity of the polarities observed for this event and for the better-constrained event no. 21, which occurred less than a day later, suggest that a strike-slip solution is more likely. Similarly, event no. 43

is not well constrained by the first-motion polarities, but a strike-slip solution is very similar to the centroid-moment tensor solution determined by Giardini *et al.* (1984).

The mechanism for event no. 8 could not, however, be dominated by strike-slip motion. McKenzie's (1972) solution for this event (the dashed nodal planes in Fig. 13) has been redrawn to eliminate several inconsistent polarities. The resultant almost pure thrust reflects a different style of deformation from the strike-slip motion occurring less than 100 km to the southwest. The NE slip vector direction for event no. 8 is similar to that in the strike-slip events, if the NE–SW striking nodal planes are chosen as the fault planes. Young structural features support this choice (Fig. 4) and it seems likely that the NE–SW trending faults in this area are now active with left lateral strike-slip motion. We are not aware of any reports of surface faulting associated with specific earthquakes in this region.

5.4.2 Serbia and Macedonia

Three other major events have occurred in inland Yugoslavia in the last 22 years. Event no. 6 (1963 July 26) occurred very close to the city of Skopje in Macedonia and has been the subject of many studies (e.g. Unesco earthquake study missions report 1968; Berg 1964; Arsovski *et al.* 1966; Ambraseys 1966). A first-motion solution for this event was determined by McKenzie (1972) and has been redrawn in Fig. 13 using a crustal velocity at the focus. No surface faulting was observed after this earthquake (Ambraseys & Morgenstern 1966) but Zatopek (1968) suggested that the aftershocks align along a NW–SE trend in the vicinity of Skopje. However, this aftershock distribution is far from clear, and Sorsky (1968), Arsovski & Hadzievsky (1970) and Arsovski (1970) report a clearly defined young zone of 'intense and sharply differentiated movements' running approximately ENE south of Skopje. The strike of the SE-dipping nodal plane in Fig. 13 is not well constrained and a solution with a more ENE striking nodal plane could be constructed. We think it likely that this earthquake involved right-lateral strike-slip motion on a SE-dipping plane with the slip vector direction approximately NE–SW. This strike is similar to that of the Scutari–Pec Line (Fig. 4) and may indicate that this feature persists as an important tectonic boundary.

Further north, a strike-slip mechanism was also determined for event no. 40 (1980 May 18). The first-motion solution is not well constrained and could also be drawn as a thrust (dashed and dotted line in Fig. 13). However, our preferred choice of a strike-slip solution is supported by the centroid-moment tensor solution of Giardini *et al.* (1984; dashed line in Fig. 13) and by another nearby strike-slip centroid-moment tensor solution (1984 September 7), which has nodal planes striking 278° and 10° and dipping 78° and 81°, respectively (Irby *et al.* 1985a). The main structural features in the epicentral region of these events follow the Dinaride trend (NW–SE), but we do not know whether the NW or NE striking nodal planes are the fault planes.

5.4.3 Dalmatian coast

The southern Dalmatian coast is the most seismically active area of Yugoslavia (Fig. 3). Earthquakes occur in a band approximately 100 km wide running south from near Split towards Albania. The historical seismicity of this area shows a similar pattern with the largest events occurring south of Split (Anderson 1985). The recent seismicity is dominated by the 1979 April 15 Montenegro event and its aftershock sequence, but two important events have occurred further north along the coast. The fault plane solution for event no. 4 (1962 January 11) was presented by McKenzie (1972), based on short-period observations from Di Filippo & Peronaci (1962). This solution is reasonably well constrained and is very

different from the almost pure dip-slip events observed farther south (Fig. 5). One of the nodal planes strikes parallel to the coast and it is tempting to assume that this one is also the fault plane. However, this choice involves a slip vector orthogonal to those observed elsewhere, and movement on the NNE striking plane is perhaps more likely.

The centroid-moment tensor solution for earthquake no. 50 (1984 May 13), south of event no. 4, shows almost pure thrusting with nodal planes striking parallel to the coast and a seismic moment of 1.69×10^{17} Nm (Dziewonski *et al.* 1985, and Fig. 5). The mechanism is very similar to those of the Montenegro earthquakes further south.

There are several studies of the Montenegro earthquake of 1979 April 15 (no. 35), its foreshocks (including no. 34) and aftershocks (including nos 36 and 37), (e.g. Academy of Sciences, Albania 1983; Hurtig & Neunhofer 1980; Console & Favali 1981). A large foreshock (no. 34, $m_b = 5.3$) occurred six days before the main shock. The first-motion solution for this event is very poorly constrained but it is important because it requires a different mechanism from the following large events (nos 35–37). A solution can be drawn (Fig. 13 dashed line) so that one of the slip vectors is parallel to those observed for the following events, but this suggests movement on a N–S striking plane for which there is no evidence from either the local tectonics or other fault plane solutions. A nodal plane with a shallow NE dip, similar to that observed in the later events can be drawn, but the slip vector on such a plane is quite different from those determined for the other events. An active fault with a NE trend has been recognised in the vicinity of the Scutari–Pec Line further south (Kociaj & Sulstarova 1980) and this foreshock might have involved motion on a fault of this strike (solid line, Fig. 13).

Several methods have been used to determine a focal mechanism for the 1979 Montenegro mainshock (event no. 35). Our first-motion solution is shown as a solid line in Fig. 13. The mechanism determined by Boore *et al.* (1981) was based on *P*-waves and *S*-wave polarization (dashed line), and the centroid-moment tensor solution of Giardini *et al.* (1984) is shown by dashed and dotted lines. A slight refinement to the solution was made using long-period surface waves (Kanamori & Given 1981) but is not presented here. The moment determined by the centroid-moment tensor method was 3.11×10^{19} Nm. A focal depth of 22 km was estimated from modelling of long-period body waves by Boore *et al.* (1981), who found that the seismic moment estimated from the amplitude of the first cycle of long-period body waves was four times smaller than that calculated from inversion of the Rayleigh waves (4.6×10^{19} Nm). This discrepancy suggests that the event was a multiple rupture.

A centroid-moment tensor solution (Giardini *et al.* 1984) for a large aftershock on the same day as the mainshock (1979 April 15, no. 36) with a seismic moment of 6.04×10^{17} Nm is shown in Fig. 5. The first motions of this aftershock were obscured and unreliable. Another large aftershock occurred more than a month later (1979 May 24, no. 37). Two solutions that are compatible with the first motion polarities are shown in Fig. 13 (solid, dashed and dotted lines). In both cases the shallow dipping nodal plane is very poorly constrained. The centroid-moment tensor solution of Giardini *et al.* (1984) is shown as a dashed line in Fig. 13 and, although there is notable inconsistency with some first motion polarities the strikes of the nodal planes are very similar. The slip vector direction is again approximately NE–SW and the moment determined for this event was 2.24×10^{18} Nm.

5.5 ALBANIA AND NORTHWEST GREECE

Both normal and thrust faulting mechanisms occur in Albania and northwestern Greece. The thrust faulting mechanisms are concentrated along coastal Albania whereas the normal

faulting events described here are at the westernmost limit of the extension in the Aegean area (McKenzie 1978; Jackson, King & Vita-Finzi 1982b).

5.5.1 Normal faulting

Four dominantly normal faulting events are shown in Fig. 5. McKenzie's (1972) mechanism for the most northern of these (no. 12; 1967 November 30) has been redrawn with a crustal velocity at the focus and additional polarity observations (Fig. 14). The WNW dipping nodal plane is well constrained but the strike of the other is not. Surface faulting in this earthquake was described by Sulstarova & Kociaj (1980). The faulting had a strike of 040° and was more than 10 km in length. However, there is some confusion over the direction of throw on this fault. Although Sulstarova & Kociaj (1980) emphasise that the strike of the surface faulting coincides with one of the nodal planes in their (apparently upper hemisphere) focal mechanism, photographs and text are ambiguous (e.g. 'All along its length

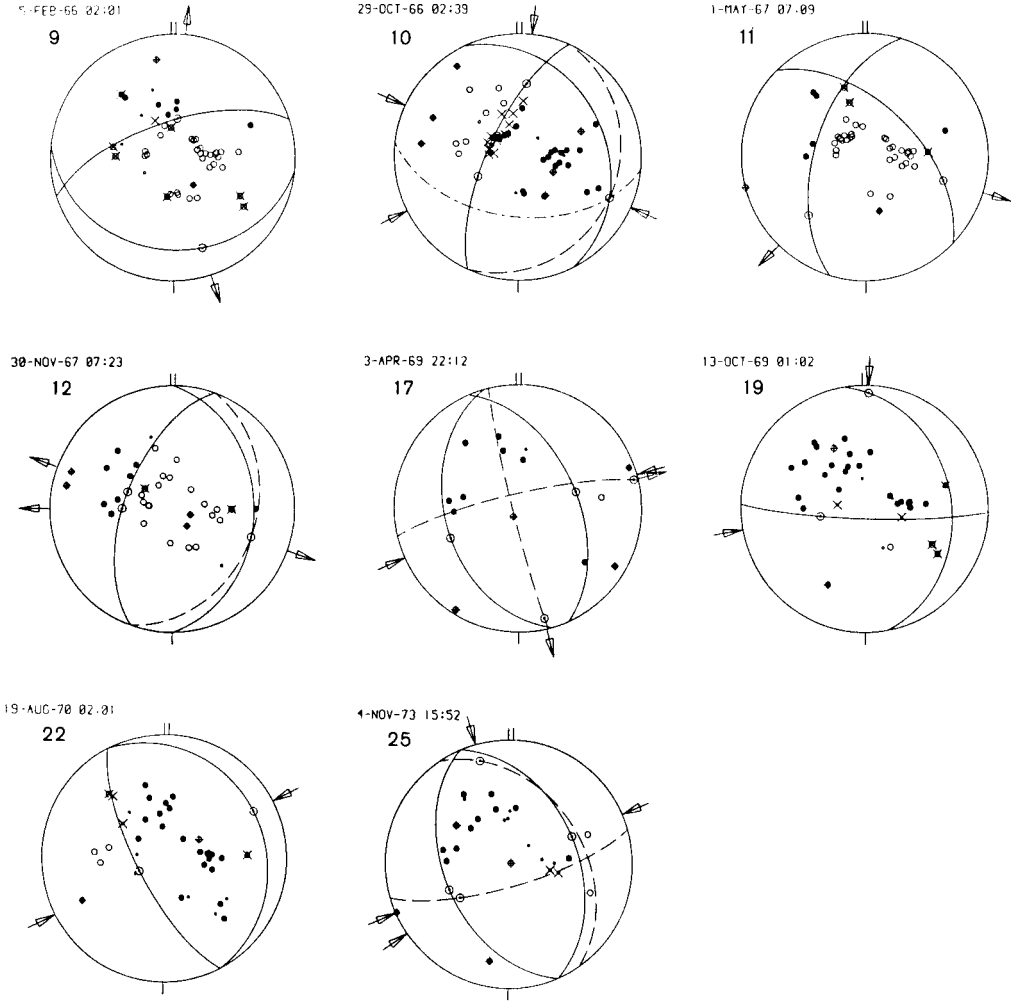

Figure 14. Fault plane solutions for earthquakes in northwest Greece and Albania. Symbols as in Fig. 6.

the northwestern block dipped against the southeastern block'). Two solutions are presented here. The preferred mechanism (solid lines) does not violate the observed compression in the eastern quadrant, but the dashed solution allows a SE-dipping plane with a similar strike to the surface faulting observed by Sulstarova & Kociaj (1980). It is not possible to identify the fault plane until the ambiguity in the field report is resolved.

An almost purely dip-slip normal mechanism was determined for event no. 51 (1984 July 9; Fig. 5) using the centroid-moment tensor method (Irby *et al.* 1985b). This earthquake was small (seismic moment 7.6×10^{16} Nm) and no further information is yet available to relate it to the regional tectonics.

Two more normal faulting mechanisms have been determined for events further south (nos 9, 11; 1966 February 5, 1967 May 1, respectively). Event no. 9 occurred very close to the Kremasta Dam in western Greece and is thought to be associated with the filling of the reservoir. The location used here was from macroseismic data (Soufleris 1980). A focal mechanism similar to that presented here (Fig. 14) was also determined by Stein, Wiens & Fujita (1982, using body- and surface-wave data), McKenzie (1972), and Fitch & Muirhead (1974). The depth of this event was estimated at 5 km from waveform modelling (Fig. 15a) and the seismic moment was about 5.0×10^{17} Nm. The depth of 5 km estimated here is much less than that of 15 km estimated by Stein *et al.* (1982) but these authors do not present sufficient waveform data for comparison with those shown in Fig. 15(a). It is interesting to note that the Koyna earthquake of 1967 December 12 in India, which is also thought to be related to reservoir filling, had a shallow focal depth of 4.5 km (Langston & Franco-Spera 1985). Both Stein *et al.* (1982) and Fitch & Muirhead (1974) suggested that the southerly dipping nodal plane was the fault plane, but this conclusion was based on either ISC or relocated aftershock depths, which are unlikely to be reliable.

McKenzie's (1972) fault plane solution for another, more northerly, normal faulting event (no. 11, 1967 May 1) has been redrawn with a crustal source velocity (Fig. 14), and placed in its macroseismic location (Soufleris 1980), which lies west of the highest Pindos mountains. No surface faulting has been reported for this event, and the approximate N–S regional tectonic trends offer no preference for choice of fault plane. Waveform modelling suggests that this earthquake nucleated at a depth of 11 km and had a moment of 1.25×10^{18} Nm (Fig. 15b).

This belt of normal faulting can only be placed in its regional context through comparison with other normal faulting earthquakes farther east in the Aegean. McKenzie (1978) and Jackson *et al.* (1982b) both discuss the Aegean seismicity and no further synthesis has been attempted in this study.

5.5.2 Thrust faulting

The belt of thrust faulting along the southern Dalmatian coast continues south along the coastal regions of Albania and northwest Greece. This area has been the site of intense historic seismic activity in the last 2000 yr. This coastal seismicity changes character south of the island of Kefallinia (Figs 4 and 5) and earthquake activity in that region is closely related to the subduction in the Hellenic Trench.

Focal mechanisms of six events from the coastal regions of Albania and western Greece are shown in Figs 5 and 14. The strike of the shallow dipping plane for the most northerly of these (no. 22, 1970 August 19) is not well constrained and is drawn here as a pure thrust. The main structural features in the vicinity of this epicentre trend approximately NW–SE, parallel to the nodal-plane strikes shown here.

It was not possible to determine a first-motion solution for event no. 44 (1982 November

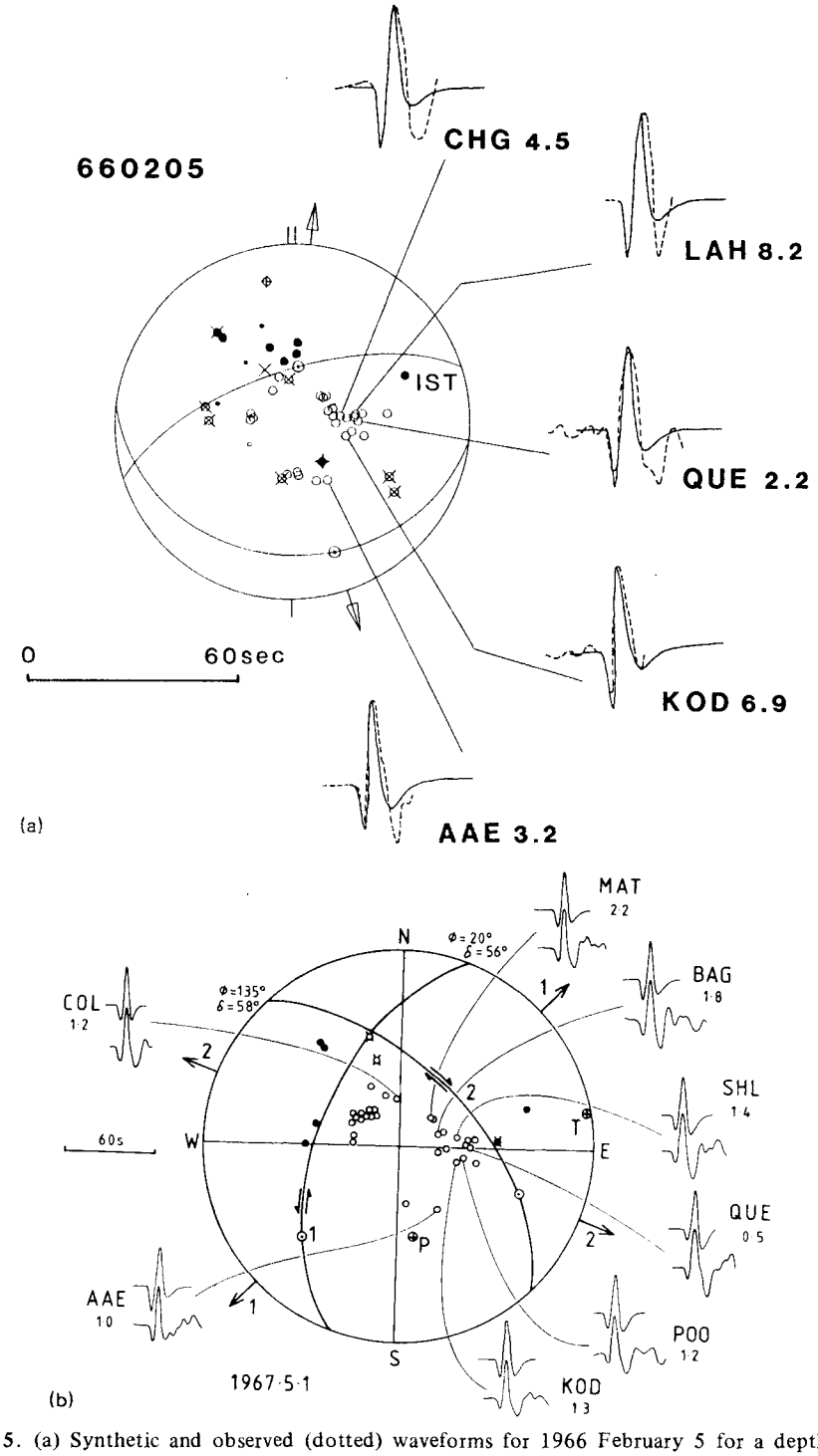

Figure 15. (a) Synthetic and observed (dotted) waveforms for 1966 February 5 for a depth of 5 km computed using a time function of 2, 0, 2 s and a velocity of 6.1 km s^{-1} above the source. WWSSN station codes and the estimated moment ($\times 10^{17}$ Nm) are shown next to each waveform pair. The average seismic moment is 5.0×10^{17} Nm. (b) Synthetic (top) and observed (bottom) long period waveforms for 1967 May 1. Synthetics are calculated at a focal depth of 11 km and moments at each station are in units of 10^{18} Nm. A time function of 2, 0, 2 s was used.

16) because almost all long-period *P*-wave onsets were confused by noise. However, a centroid-moment tensor solution has been determined by Giardini *et al.* (1984) and is shown in Fig. 5. The seismic moment for this event was 3.2×10^{17}Nm. The mechanism shows predominantly thrust faulting with a strike compatible with regional trends.

Event no. 17 (1969 April 3) has been included because Sulstarova (1980) and Aliaj (1982) reported surface faulting related to this event. Aliaj (1982) suggests that movement took place on a NNW trending fault and Sulstarova, Kociaj & Aliaj (1982) report that they 'measured the length of surface faults and dimensions of the pleistoseismal zones' of earthquakes including event no. 17, although they do not present any details. Sulstarova (1982) gives a strike-slip solution for this event (shown as a dashed line in Fig. 14). Only a limited number of long-period first-motion polarities were large enough to be read with confidence, and these are shown in Fig. 14 along with nodal planes indicating pure thrusting, which is compatible with these polarities and with the observed fault trend striking NNW mentioned by the Albanians. Several of these polarities are incompatible with the solution of Sulstarova (1982), so it seems likely that this event, like others in this part of Albania, involved thrust faulting on a NW-striking fault plane.

A fault plane solution for event no. 19 (1969 October 13) was published by McKenzie (1972), but the wrong epicentral location was used for calculating the position of stations on the focal sphere. The solution in Fig. 14 has been recalculated at the macroseismic epicentre (Soufleris 1980) and uses additional polarity observations. The strike of the shallow-dipping plane is not well constrained but can be constructed to give a slip vector on the steep plane that is similar to those in nearby thrusting events. Although E–W, apparently left lateral, strike-slip faults of Tertiary age are known in this part of western Epirus (I.F.P. 1966), they are not well dated and there is no direct evidence of their recent reactivation, even by microearthquakes (King *et al.* 1983).

Another, relatively poorly controlled, focal mechanism has been determined for an event (no. 25, 1973 November 4), which occurred offshore at the junction of the Albanian thrust belt and the Hellenic Trench (Figs 5 and 16). Two alternative solutions are shown in Fig. 14. The predominantly thrust faulting solution (also shown by McKenzie 1978) is similar to those further north, but a large component of strike-slip could also be involved. However, if movement occurred on a NE-striking fault then this would require left-lateral strike-slip, as opposed to the right-lateral movement on NE striking faults shown by better constrained solutions further south (nos 24 and 26). We therefore think that the thrusting solution is more likely.

Ambraseys (1975) observed surface faulting of an ambiguous nature that might be associated with event no. 10 (1966 October 29), and although the shallow-dipping plane is unconstrained in the focal mechanism (extremes shown as dashed or dot-and-dashed lines in Fig. 14), it can be constructed with a NNW strike, parallel to the surface faulting, without violating any of the observed polarities. The fault observed by Ambraseys had a length of between 2 and 4 km and a maximum vertical displacement of 0.4 m (Fig. 16). If this really was the causative fault, the slip vector determined from the fault plane solution (Fig. 14) trends 113°, which is unlike other thrusting events further north along the Albanian coast. Both this event and no. 19, occurred in a zone between the inland normal faulting and the coastal belt of thrusting, and where complicated faulting might perhaps be expected.

The additional focal mechanisms presented here support the earlier assertion of McKenzie (1978) that the boundary separating the normal and thrust faulting in this area is apparently very sharp. McKenzie (1978) suggested that the complete change in stress orientation could be explained by the detachment and sinking of the lower part of the lithosphere beneath the thickened thrust zone. This model suggests a very limited area of compression along the

Albanian coast, but the zone of thrusting clearly continues much further north along the Yugoslavian coast (where there is no active inland belt of extension).

5.6 NORTHWEST HELLENIC SUBDUCTION ZONE

The region of the Ionian islands (Fig. 16) marks the northwest termination of the Hellenic subduction zone. Although there is no clear bathymetric expression of the subduction zone at its NW extremity (near the island of Kefallinia) the locations of large earthquakes and their mechanisms help in defining the actively deforming zone.

The locations of the events described in this section are shown in Fig. 16 and the mechanisms for which polarity information is available are shown in Fig. 17.

The two most northerly earthquakes in this zone occurred just to the west of Kefallinia and their epicentres lie above the steep-sided NNE–SSW trending bathymetric feature; the Kefallinia Valley (Fig. 16). The focal mechanism for no. 24 (1972 September 17) was shown by McKenzie (1978) as a pure dip-slip thrust. This is incompatible with several additional

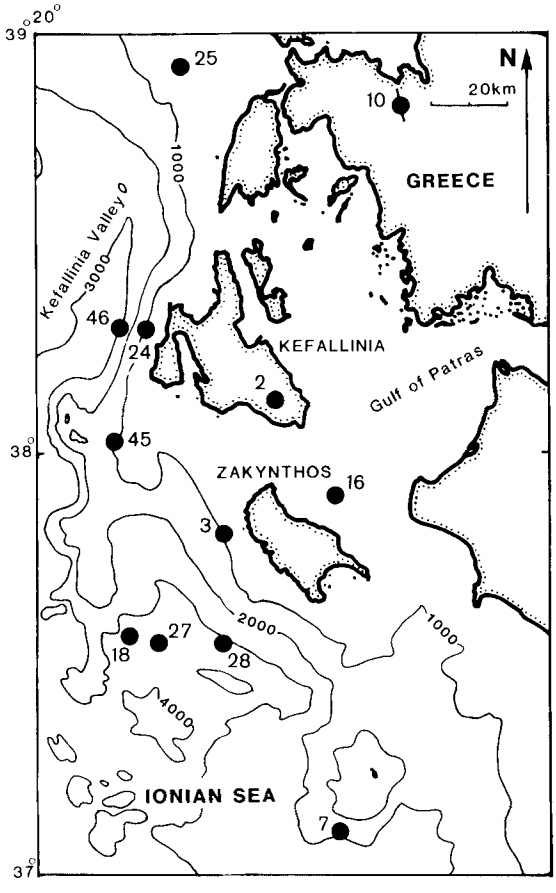

Figure 16. Bathymetric map of the NW end of the Hellenic Trench, showing the epicentres of recent large earthquakes (numbered as in Table 1). The strike of surface faulting found by Ambraseys (1975) and possibly related to event 10 is shown by a line through its epicentre. Bathymetry is from the International Bathymetric chart of the Mediterranean, UNESCO, 1981.

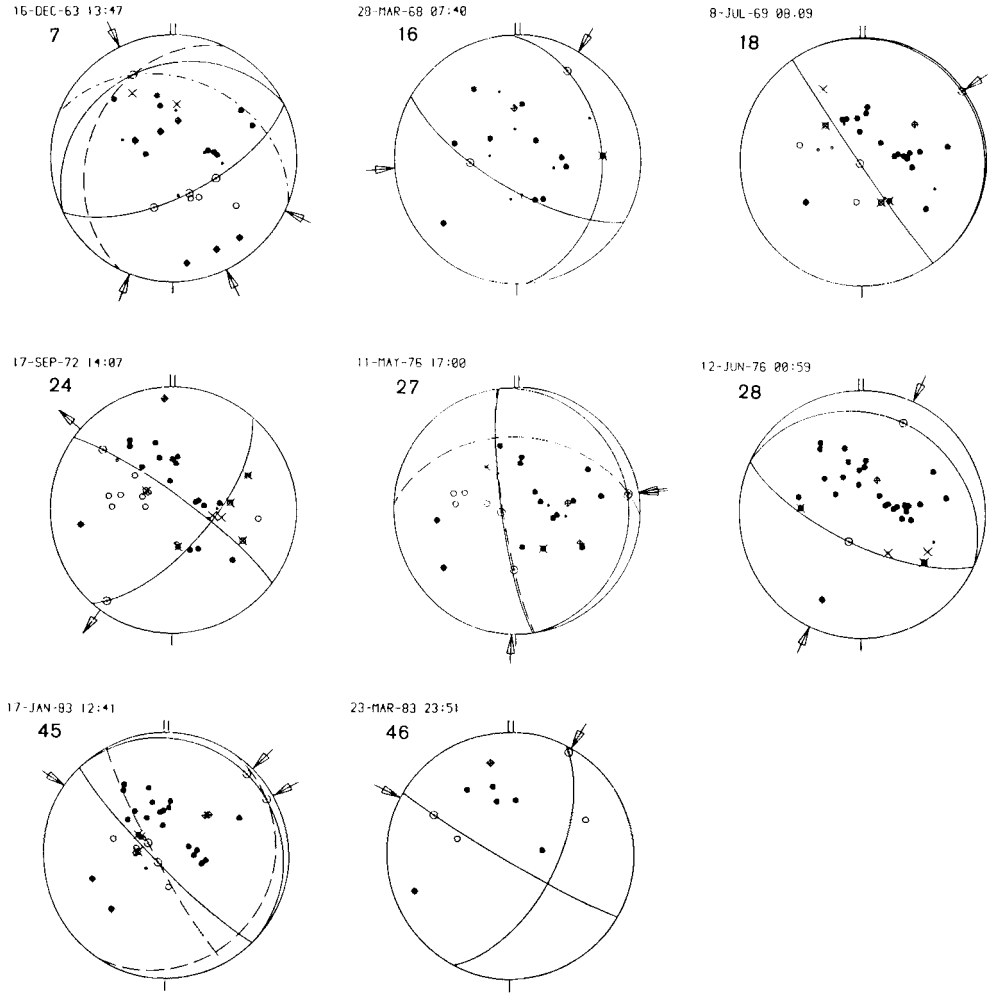

Figure 17. Fault plane solutions for earthquakes associated with the Hellenic Trench in western Greece. Symbols as in Fig. 6.

first motions that have become available, which require a well constrained strike-slip solution (Fig. 17). The NE-trending nodal plane is approximately parallel to the trend of the Kefallinia Valley, and we suspect that this mechanism involved right-lateral strike-slip in this direction. The centroid-moment tensor solution for the nearby event no. 46 (1983 March 23) is very similar, and compatible with the few polarity observations so far available (Fig. 17). The seismic moment determined by Dziewonski, Friedman & Woodhouse (1983) was 2.23×10^{18} Nm. This mechanism also suggests motion on a right-lateral strike-slip fault that probably terminates the Hellenic subduction zone.

The epicentre of event no. 45 (1983 January 17) also appears to lie on the southern extension of the steep bathymetric slope marking the eastern edge of the Kefallinia Valley. However, a strike-slip mechanism cannot easily be drawn for this earthquake. The strike of the shallow dipping nodal plane is not well controlled and the mechanism here (Fig. 16) is drawn as a pure dip-slip thrust. A centroid-moment tensor solution has also been determined for this event (dashed line in Fig. 16) and although there are some discrepancies with the

observed first-motion polarities, the solution has very little strike-slip component. This is the most northern event whose mechanism shows shallow angle thrusting of the Ionian Sea beneath Greece. Similar thrusting mechanisms for the nearby events nos 2 and 3 (1953 August 12 and 1959 November 15) were presented by McKenzie (1972) and are shown in Fig. 5, but their locations could be in error by as much as 50 km and either or both could reflect movement on thrust faults such as those observed on Kefallinia or Zakynthos (Mercier *et al.* 1976, 1979).

One recent event appears to have occurred east of Zakynthos (no. 16, 1968 March 28). Its mechanism is not well constrained but polarity observations allow nodal planes striking NW, parallel to the fault strike observed on Kefallinia by Mercier *et al.* (1976) and in the offshore eastern basin (Brooks & Ferentinos 1984).

Three events close together south of Zakynthos (nos 18, 27, 28; 1969 July 8, 1976 May 11, 1976 June 12) also have dominantly thrusting fault-plane solutions (Fig. 17). In all of these solutions the shallow dipping nodal plane is unconstrained and so all these mechanisms are shown here as pure dip-slip events. An alternative solution is shown for event no. 27, but it is likely that all these mechanisms involved thrusting of the Ionian Sea beneath Greece.

The most southerly event included in this study (no. 7, 1963 December 12), is problematic. The three dilatational first motions in the SE quadrant (Fig. 17) preclude a mechanism similar to the others described here unless the northerly dipping nodal plane has a more E–W strike than shown. Two solutions with maximum strike slip components for this event are shown in Fig. 17 and, since there is no evidence for either, a pure dip-slip thrust is shown. This mechanism is not easily compatible with any regional interpretation but, because it is clearly different from the other thrusting events to the north, may indicate motion on a transverse structure in the Hellenic Trench.

5.7 MESSINA EARTHQUAKE (1908 DECEMBER 28)

The 1908 December 28 Messina earthquake (event no. 1) is important because it is the only large recent event in the Calabria–Sicily region of southern Italy for which we have evidence of a normal faulting mechanism. In spite of its occurrence at a time when there were few seismological observatories operating, at least two focal mechanisms have been determined for this event (Fig. 5, Gasparini *et al.* 1982; Schick 1977). Neither is particularly well constrained but both require dominantly normal faulting. This event is clearly unrelated to the Tyrrhenian Benioff Zone since thrust faulting would be expected if subduction were still occurring; it has a completely different mechanism from other events in Sicily and is quite different in orientation from other normal faulting events in peninsular Italy.

The earthquake was large (magnitude 7, Schick 1977) and produced a sizeable tsunami (maximum 10.6 m, Ryan & Heezen 1965) but no surface faulting. However, a spirit levelling survey had been completed a few months before this earthquake and was repeated immediately after it. These measurements were interpreted by Mulargia & Boschi (1982) to show a strong net subsidence of the Messina Strait area. From analysis of the same geodetic data, Schick (1977) suggested that the earthquake occurred on a NE–SW trending fault running through the Messina Strait. Recent tectonic features in the Calabrian area have a similar trend (Fig. 4) and are quite different in orientation from those faults in the rest of peninsular Italy.

This earthquake therefore suggests that compressional tectonics related to subduction are not occurring in the Calabria region. Its mechanism is different from those of the nearby Sicilian events, and so it cannot be interpreted as directly reflecting the African–Eurasian collision. As in Albania and NW Greece, the boundary between this area of normal faulting

and the nearby thrusting is very sharp and probably marks an important change in stress orientation.

5.8 SUMMARY

The fault-plane solutions in the circum-Adriatic region show a clear pattern. West of Messina, thrust faulting occurs with slip vectors that appear to reflect the overall motion between Africa and Eurasia (Fig. 5). In peninsular Italy only normal faulting mechanisms are found, but these change to pure dip-slip thrusting at the northern end of the Adriatic Sea. Inland northern Yugoslavia shows strike-slip and thrusting mechanisms, and inland strike-slip activity is also seen in southern Yugoslavia. Along the southern Dalmatian coast thrusting occurs on shallow landward-dipping faults. This thrusting continues south along the coast of Albania and northwestern Greece as far as Kefallinia. In this region, the bathymetry, the lack of intermediate depth earthquakes further north, and two right-lateral strike-slip mechanisms suggest that thrusting in the Hellenic subduction zone terminates against a strike-slip fault. South of Kefallinia, thrust faulting associated with subduction of the Mediterranean beneath the Aegean plate dominates the seismicity. The normal faulting in the Aegean extends slightly west of the highest topography in the Pindos mountains into Albania and NW Greece. The normal faulting in the 1908 Messina earthquake is not obviously related to either the Africa–Eurasia convergence, or to active subduction in the Tyrrhenian Benioff Zone, or to the normal faulting observed elsewhere in peninsular Italy.

6 Motion of the Adriatic block

The normal faulting in peninsular Italy cannot be explained in terms of the Africa–Eurasia convergence. As shown in Fig. 2, the slip vector azimuths in central Italy should be NNW if they represent movement about the Africa–Eurasia pole. Similarly, if thrusting in Yugoslavia were related to the Africa–Eurasia motion, then the slip vector should also be NNW: approximately orthogonal to that which is observed. Fig. 18 shows a summary of the slip vector directions derived from the well constrained focal mechanisms discussed in this paper, together with those predicted for the Africa–Eurasia convergence.

Several groups of slip-vector orientations can be recognized. The N–S slip vectors observed in Sicily match reasonably those predicted for the Africa–Eurasia convergence. Those south of Kefallinia are related to subduction in the Hellenic Trench. The slip vectors of normal faulting earthquakes in Albania and NW Greece are not shown in Fig. 18, but are presumably related to the extension in the Aegean. Slip vector azimuths along the Yugoslavian and Albanian coasts appear to change in the Montenegro area.

Perhaps the most striking feature of the seismicity in this region is the lack of activity in the Adriatic Sea itself. A few small, scattered earthquakes do occur in the Adriatic, particularly near the Gargano Ridge (Figs 3 and 4), but the activity is very much less intense than in the surrounding mountain belts: a feature that is reflected in the bathymetry of the Adriatic, which is relatively flat. The larger earthquakes occur almost entirely in coastal or land areas, as seen from the locations of the earthquakes for which teleseismic first-motion fault-plane solutions are available (Fig. 5); which necessarily have magnitudes greater than about $m_b = 5.2$. This pattern is also seen in the historical seismicity of the region (Anderson 1985). We believe that the absence, or low levels, of deformation in the Adriatic Sea indicate that its behaviour is that of a relatively rigid block within the deforming region, similar to that of Central Turkey, the southern Caspian Sea and central Iran further east (Jackson & McKenzie 1984). It should therefore be possible to describe its motion relative to the

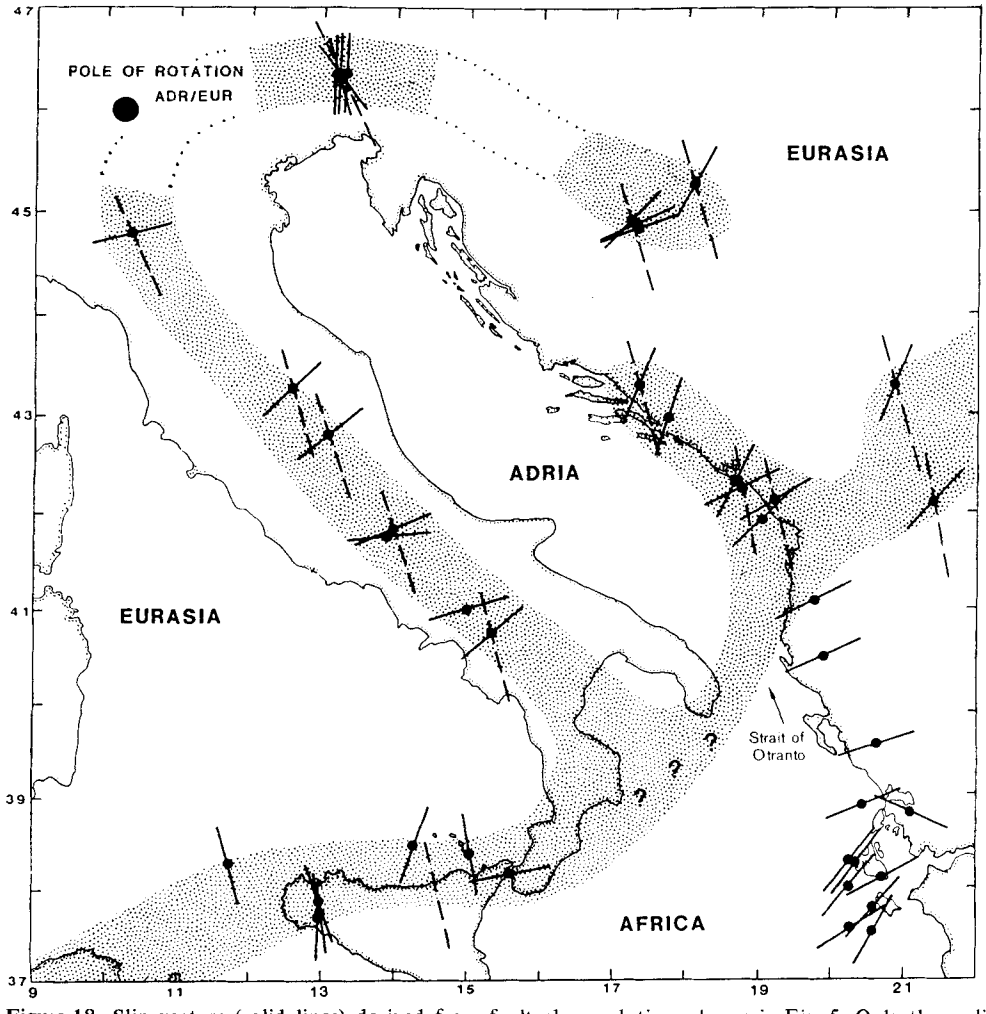

Figure 18. Slip vectors (solid lines) derived from fault plane solutions shown in Fig. 5. Only those slip vectors that are reasonably well defined by the fault plane solution are shown. Dotted lines indicate the azimuth of slip vectors expected for movement about the African–Eurasian pole. In central Italy and Yugoslavia the observed slip vectors are at a high angle to the Africa–Eurasia direction and their orientations define an Adria–Eurasia pole of rotation at about 45.8°N, 10.2°E in northern Italy. Shaded areas indicate the seismically active borders of Adria which connect with the deformation zone between Africa and Eurasia in northern Sicily. The location of the Adria-Africa boundary is uncertain but the presence of some seismicity in the Strait of Otranto (Fig. 3) suggests that it may occur in this region. The more easterly azimuth of slip vectors along the Albanian coast and in the Messina Strait may indicate deformation associated with the Africa–Adria boundary but this cannot be conclusively demonstrated.

Eurasian plate by a rotation about an Eulerian pole, and we will now use the slip vectors of earthquakes in the deforming belts surrounding the Adriatic to help define such a pole. It is important to appreciate the reasons for undertaking such an exercise, which are (i) to see whether rotation about a pole can account in a general way for the change in style and orientation of faulting around the boundaries of the Adriatic Sea, and (ii) to use the pole to predict the overall rate and orientation of motion across the 100–200 km wide deforming belts that surround the Adriatic Sea. We do not believe that the slip vectors on all the faults in these wide deforming zones will reflect the motion predicted by the pole of rotation, in

the way expected within the narrower zones of deformation that bound plates in the oceans. Faulting in the wider deforming zones that bound relatively rigid continental blocks is distributed, may involve complicated geometries, and the overall resultant deformation is best described by a continuum approach (see McKenzie & Jackson 1983; Jackson & McKenzie 1984; Walcott 1984). However, in order to predict features of the continuum deformation, such as crustal thickening and palaeomagnetic rotations, and in order to investigate how faulting is able to take up the distributed deformation, the velocity boundary conditions across the deforming zone must be known (see e.g. Walcott 1984; McKenzie & Jackson 1986); these can usefully be predicted by the relative motion of the stable blocks on either side, which is described by a rotation about a pole.

The most important constraint on the location of the Eurasia–Adria pole is the slip vector azimuth of the Friuli events. This direction is identical to that predicted by Africa–Eurasia convergence (Fig. 18), and might imply a continuity of the Adriatic block with Africa (as a 'promontory'). However, the deforming margins of this block, in Italy and Yugoslavia, should then be deforming with the NNW slip vectors shown by the dashed lines in Fig. 18. They are not. Since the belt of seismicity surrounding the Adriatic is continuous, then the Friuli events cannot reflect African–Eurasia convergence and must be part of the Adria–Eurasia motion.

An instantaneous pole of rotation has therefore been calculated using the Friuli slip vectors and the slip vectors of other central Italian and coastal Yugoslavian events. The observed and calculated slip vector azimuths for the best fitting pole of rotation, located in

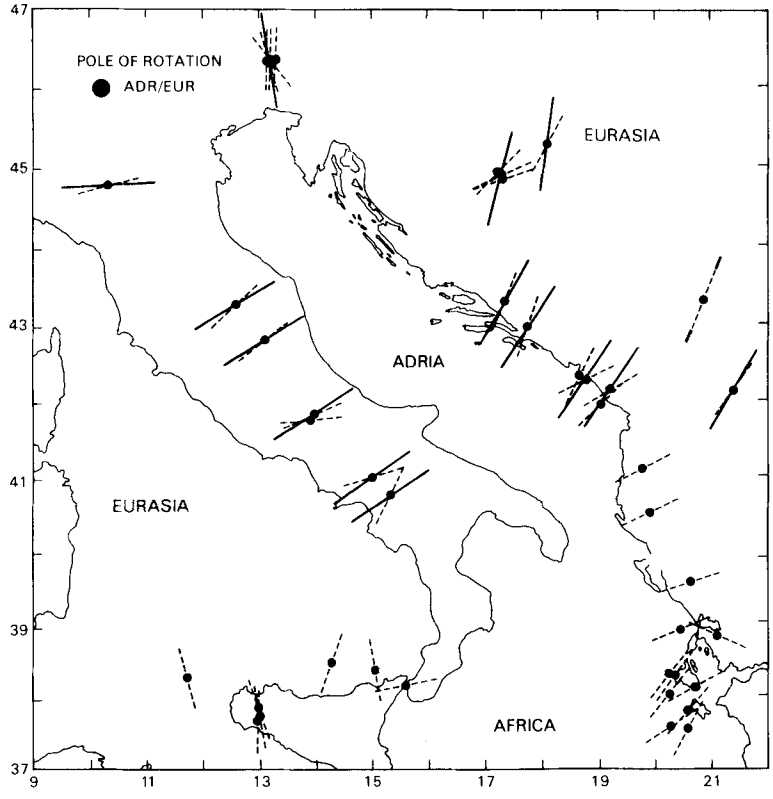

Figure 19. Comparison of observed slip vectors from fault plane solutions (dotted lines) and slip vectors calculated from a pole of rotation at 45.8° N 10.2° E between Adria and Eurasia (solid lines).

northern Italy at 45.8°N, 10.2°E, are shown in Fig. 19. Calculation of this pole did not include the four events in the Pannonian Basin (nos 8, 20, 21, 43) or the two events in Macedonia (6, 40) which may not be representative of the Adria–Eurasia motion. However, inclusion of these six events makes little difference; the resulting pole being at 46.0°N 10.2°E. Inclusion of the coastal Albanian events (17, 44) gives a pole of 46.2°N, 10.4°E, but the misfits to these slip vectors are between 20° and 30°, and it is unlikely that they occurred on part of the deforming Adriatic margin.

The obvious question then is: where are the boundaries of Adria? The wide belt of seismicity running through Italy round the Alps and down through the Dinarides obviously marks the deforming edges of the Adriatic rigid block which is rotating anticlockwise about a pole in northern Italy. This seismicity marks the boundary with Eurasia but there is no evidence for the location of the Adria–Africa boundary. It must lie between Sicily and the Campania region of peninsular Italy, and probably crosses the Balkan coastline south of Montenegro. Although some historical seismicity is known from the Gargano Peninsular region (41.5°N 15.8°E), such as the moderate earthquake of 1627 (Molin & Margottini 1984), the southern part of the Apulia–Gargano region appears relatively aseismic and seems to be part of the stable Adriatic zone, so the Africa–Adria boundary probably lies to the south of this region. One possible boundary zone is indicated in Fig. 18. Very few earthquakes have been located in this zone but a small cluster of events in the Strait of Otranto may be important. None of these events was large enough for a fault-plane solution to be determined, but they may mark the site of future important events.

Since the Africa–Adria boundary is not marked by intense seismic activity it seems probable that the relative motion between the African plate and the Adriatic block is small. The relative motion between Africa, Eurasia and Adria can be compared at the Strait of Otranto. Fig. 20 shows the velocity triangle for this area in which Africa is moving NNW relative to Eurasia at a rate of 8.8 mm yr^{-1}. Adria is moving in a NE direction relative to Eurasia at an unknown rate. If the relative motion between Africa and Adria is to be

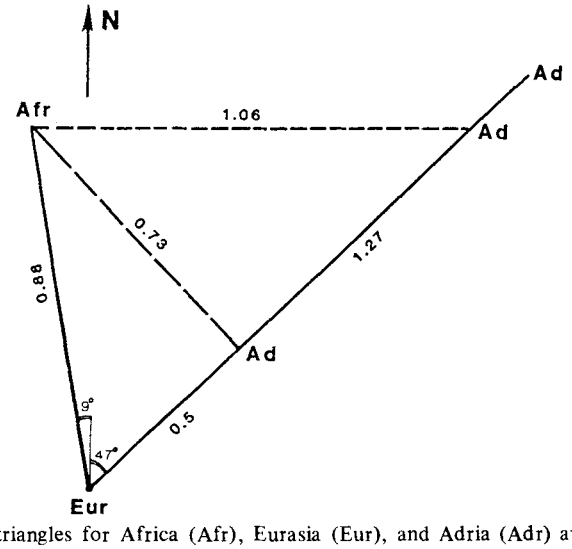

Figure 20. Velocity triangles for Africa (Afr), Eurasia (Eur), and Adria (Adr) at the Strait of Otranto. Velocities are shown in cm yr^{-1}. The Adria–Africa motion is uncertain because only the direction and not the magnitude of the velocity of Adria with respect to Eurasia is known. Possible relative motions between Adria and Africa are shown as dashed lines. The Africa–Eurasia motion is determined from rotation about the pole shown in Fig. 2 with an angular velocity of 1.42×10^{-7} deg yr^{-1}, derived by Chase (1978).

minimized, then Adria moves SE relative to Africa at a rate of about 7.3 mm yr^{-1}. This would require an Adria–Eurasia velocity of 5.0 mm yr^{-1}. An alternative possibility is that, because the Adria–Eurasia deforming zone is the most seismically active, the velocity of Adria relative to Eurasia is greater than both the Africa–Eurasia and the Adria–Africa rates. Increasing the Adria–Eurasia velocity to 12.7 mm yr^{-1} predicts an E–W relative motion between Adria and Africa in this area, which is similar to the slip vector in the Messina earthquake, and thus the paucity of seismicity might reflect a major strain release associated with this earthquake. There is, however, no way to define the motion of Africa relative to Adria unless either the rotation rate of the Adria–Eurasia motion or a focal mechanism for an earthquake clearly related to the Africa–Adria motion can be determined.

7 Rates of deformation

In this section we use Kostrov's (1974) result that the average tensor strain rate $\dot{\bar{\epsilon}}_{ij}$ across a deforming zone can be obtained by summing the seismic-moment tensor elements M_{ij} of N earthquakes within the zone. Thus

$$\dot{\bar{\epsilon}}_{ij} = \frac{1}{2\mu V \tau} \sum_{n=1}^{N} M_{ij}^{n},$$

where μ is the rigidity, V the volume of the deforming zone, M_{ij}^{n} is the moment tensor of the nth earthquake, and τ the time interval over which the moment tensors are summed.

We obtained the six elements of the seismic moment tensor for each first motion fault plane solution using the relation

$$M_{ij} = M_0(u_i n_j + u_j n_i),$$

where M_{ij} is the moment tensor, M_0 the scalar moment, and $\hat{\mathbf{u}}$ and $\hat{\mathbf{n}}$ are unit vectors in the direction of the slip vector and the normal to the fault plane, respectively (see Aki & Richards 1980). The coordinate frame used was with the y = north, x = east and z = up directions positive. For many of these earthquakes, the scalar moment could only be determined from a moment-magnitude relationship. Dziewonski & Woodhouse (1983) determined a relationship between surface wave magnitude and moment of:

$$M_s = 0.668 \log M_0 - 10.86,$$

where M_0 is in dyne – cm (1 dyne – cm = 10^{-7} Nm).

The errors in the calculation of surface-wave magnitude and in the moment-magnitude relationship are difficult to assess. The equivalent moment values for surface wave magnitudes of 5.8 and 6.0 are 8.7×10^{17} Nm and 1.7×10^{18} Nm, respectively, so an error of 0.2 in the M_s value determined in this range produces a factor of two difference in the moment value. Because the relation is logarithmic, the errors in the moment assessment of the thirteen largest earthquakes in the Adriatic seismic belt are probably much greater than the sum total of all the smaller events. Therefore, only the largest events were considered in our calculations. The moment tensor elements of these events are shown in Table 4.

The summed seismic-moment tensor elements for central Italy and coastal Yugoslavia are also shown in Table 4. The magnitudes of the individual moment tensor elements are very similar in these two areas, which they should be if central Italy and coastal Yugoslavia are opposing deforming margins of the relatively aseismic Adria. A similar result was obtained in a study of the twentieth century seismicity of the region by Anderson (1985). She used a moment-magnitude relation to estimate static seismic moment (M_0) rates for central Italy and Yugoslavia of 15 and 22×10^{17} Nm yr^{-1}. Table 4 also shows the summed moment

Table 4. Seismic-moment tensor elements.

Event no.	Date	M_0 ($\times 10^{18}$ Nm)	M_{xx}	M_{yy}	M_{zz}	M_{xy}	M_{xz}	M_{yz}
Central Italy								
23	71.07.15	0.1	0.0	0.0	0.0	0.1	0.0	0.1
47	84.04.29	0.3	0.1	0.1	−0.2	0.1	−0.1	−0.2
38	79.09.19	0.7	0.7	−0.4	−0.3	0.1	−0.1	−0.4
48	84.05.07	0.8	0.5	0.1	−0.6	0.3	−0.3	−0.5
49	84.05.11	0.2	0.1	0.1	−0.2	0.1	0.0	0.0
5	62.08.21	0.7	0.4	0.1	−0.5	0.3	−0.2	−0.4
42	80.11.23	26.0	7.4	13.9	−21.2	10.9	−11.9	−8.2
Sum:			9.2	13.8	−23.0	11.8	−12.6	−9.6
Coastal Yugoslavia								
4	62.01.11	6.0	−3.8	2.7	1.1	−3.9	−2.5	1.7
50	84.05.13	0.2	0.0	−0.1	0.1	0.0	0.0	−0.2
35	79.04.15	46.0	−8.5	−18.5	27.0	−12.6	−18.7	−32.1
37	79.05.24	2.2	−1.1	−0.3	1.4	−0.6	−1.5	−0.7
36	79.04.15	0.6	0.0	0.0	0.0	0.0	−0.5	−0.3
34	79.04.09	0.1	0.0	0.0	0.0	0.0	−0.1	0.0
Sum			−13.5	−16.1	29.6	−17.2	−23.4	−31.7

Moment tensors rotated to the frame x = azimuth 122°, y = azimuth 032°, z = vertical (positive):

$$\begin{bmatrix} -0.1 & 3.1 & -5.6 \\ & 23.1 & -14.8 \\ & & -23.0 \end{bmatrix}$$

Italy

$$\begin{bmatrix} 1.2 & -6.4 & -3.0 \\ & -30.8 & -39.3 \\ & & 29.6 \end{bmatrix}$$

Yugoslavia

tensors for Italy and Yugoslavia rotated into a new coordinate frame, in which the axes x_1, x_2, x_3 are positive in the directions 122°, 032°, and vertical. In this frame the x_2 direction is normal to the strike of the deforming belt in central Italy. The rate of seismic extension across this zone is given by

$$v_2 = \frac{1}{2\mu l t \tau} \sum_{n=1}^{N} M_{zz}^n,$$

(see Kostrov 1974; Jackson & McKenzie 1987), where l is the length of the deforming zone along strike and t is its seismogenic thickness. For central Italy, taking $l = 420$ km, $t = 15$ km, $\mu = 3 \times 10^{10}$ Nm^{-2} and $\tau = 21$ yr gives an estimated extension velocity of 2.9 mm yr^{-1}. This velocity normal to the strike of the deforming zone (in azimuth 032°) is the only one predicted by the motion of the 'rigid' blocks either side (see Jackson & McKenzie 1987). However, the pole of rotation between Adria and Eurasia found in section 6 predicts an overall direction of motion across the zone in central Italy of 058°. Thus, to have a resolved component in the direction 032° of 2.9 mm yr^{-1}, the overall motion between Adria and Eurasia would have a magnitude of 3.2 mm yr^{-1}. In coastal Yugoslavia, using values of $l = 250$ km, $t = 15$ km and $\tau = 21$ yr, the seismic shortening normal to the zone (azimuth 032°), which is similar in direction to the overall Adria–Eurasia motion predicted by the pole of rotation in Section 6 (azimuth 034°) is calculated to be 6.5 mm yr^{-1}. Both these rates are uncertain by at least a factor of two, are dominated by the contribution of the largest earthquakes in the 21 yr period concerned (no. 42 in Italy and no. 35 in Yugoslavia), and ignore the unknown contribution of aseismic creep to the

overall deformation. However, the rates calculated using a 21 yr seismicity are similar in magnitude to those found by Jackson & McKenzie (1987) using a 70 yr seismicity: they estimated seismic extension rates of 1.3–3.5 mm yr^{-1} in central Italy and seismic shortening of 1.0–2.4 mm yr^{-1} in coastal Yugoslavia.

Predicted velocities between Adria and Eurasia in the strait of Otranto are roughly double those in central Italy (because of the increased distance from the pole of rotation). The Adria–Eurasia velocities estimated from the seismicity above are similar in magnitude to those shown in the tentative velocity triangles for the Strait of Otranto in Fig. 20. However, their considerable uncertainty, combined with the unknown contribution of aseismic creep, does not allow them to help in solving the enigma of the Africa–Adria boundary. This boundary is not defined by a belt of intense seismicity, so its nature and location are uncertain (Fig. 18). The slip vector in the Messina earthquake (Fig. 5) was approximately E–W, and may represent deformation in the Adria–Africa boundary zone. However, such a suggestion is very tentative and must await further evidence in the form of large earthquakes in the Ionian Sea, Calabria or Strait of Otranto.

8 Discussion

It is now possible to demonstrate that the current deformation in the Adriatic area is not simply reflecting the N–S shortening between Africa and Eurasia. This was suggested by McKenzie (1972), but there were insufficient good focal mechanisms to demonstrate it conclusively at that time. The slip vectors of 24 fault-plane solutions show that the bulk movement of the relatively stable Adriatic block can be approximated by an anticlockwise rotation relative to Eurasia about an Eulerian pole at 45.8°N, 10.2°E. The current extensional deformation in Italy and the thrusting in northern Italy and Yugoslavia therefore reflect the deforming margins of the relatively aseismic Adriatic area.

An alternative view might be that the Adriatic Sea is still attached to Africa in some sense but deforms internally: slip vectors within the deforming region would then not be required to reflect the overall Africa–Eurasia motion. We feel this view is unnecessarily complicated and does not explain why (a) the observed slip vectors match those predicted by the rotation about a pole in N. Italy (Fig. 19), and (b) the seismicity is concentrated in the land and coastal areas, which are generally mountainous, while the sea-floor is relatively flat and aseismic. This alternative view requires that the Adriatic Sea deforms dramatically by creep and yet produces no substantial topography or bathymetry. It also begs the question: to what extent is it meaningful to consider the Adriatic Sea as a promontory of Africa if it is not rigid but deforms internally? We feel that the description we offer, in which the Adriatic Sea acts as an effectively rigid block rotating relative to Eurasia about a pole in N. Italy, describes the general nature of the deformation in the wide deforming belts separating the Adriatic and Eurasia in a far simpler way.

Unlike many of the other western Mediterranean basins, the Adriatic Sea area is underlain by continental crust that is typically 25–36 km thick and reaches a maximum of 35–40 km thickness beneath the southern Adriatic basin (Dragasevic 1973; Nicholich 1981). An important lithospheric discontinuity in the Gargano Ridge area is also suggested by Calcagnile & Panza (1981). From inversion of the regional dispersion relations derived from surface waves, combined with the results of crustal refraction surveys, they recognize a change in the lithospheric thickness from about 70 km in the northern Adriatic basin to more than 110 km in the southern Adriatic basin. A scattered band of weak seismic activity crosses the central Adriatic Sea (Fig. 3) near the Gargano Ridge. The change in crustal and lithospheric structure in this area may mark some internal deformation of the Adriatic

block; possibly a relic of the former behaviour of the Adriatic block as a 'promontory of Africa'.

Recent interpretations of palaeomagnetic data by Vandenberg (1983) and Vandenberg & Zijderveld (1982) suggest that the Italian peninsula, Sardinia and the southern Alps formed a single 'Adriatic continental block' which rotated twice: once during the Late Cretaceous as a northern promontory of the African plate, and for a second time, independently from Africa and Europe, in the post-Early Tertiary. The focal mechanisms presented here show that this recent anticlockwise rotation, which has amounted to about 30° since the Early Tertiary, is still continuing.

Finally, we should stress that the kinematics discussed in this paper, because they are based on earthquake mechanisms, are restricted solely to a description of present-day motions. These need not be representative of longer term motions and the kinematics described here are unlikely to be the same as those prior to the Pliocene. The pre-Pliocene deformation of this area is certainly complicated (see Mantovani, Babbucci & Farsi 1985, among others) and probably involved motions different from those occurring today.

9 Conclusions

This study demonstrates that in the Adriatic region, as elsewhere in the Alpine–Himalayan seismic belt (e.g. Molnar & Tapponnier 1981; Jackson & McKenzie 1984), there is a large continental block in which the seismicity is relatively feeble. The relative rigidity of this block allows its bulk motion to be described by rotation about a pole, and goes some way towards accounting for the differences in slip vector directions, deformation style and levels of seismicity around its boundaries.

The N–S shortening in Sicily changes to NE–SW extension in peninsular Italy, which in turn changes to thrusting in N. Italy. A belt of active shortening exists from N. Italy southwards along the Yugoslavian and Albanian coasts, and into Greece. The superior data of the last 21 years support the suggestion from all the 20th Century seismicity; that the extension rate in southern peninsular Italy and the shortening rate in southern coastal Yugoslavia are about equal. The seismicity accounts for about 2.0 mm yr^{-1} of motion in these regions, but the velocity may be much greater if aseismic creep contributes substantially to the deformation. Thus the Adriatic Sea is surrounded by belts of high topography and seismicity that are about 100–150 km wide. The new set of fault-plane solutions presented here strongly support the suggestion that the Adriatic region has become detached from the African continent. The boundary between Adria and Africa is not marked by a belt of intense seismicity but may be located in the southern Adriatic Sea, near the Strait of Otranto.

Acknowledgments

This work was supported in part by a grant from the Natural Environment Research Council. H.J.A. acknowledges a postgraduate funding award from the New Zealand National Research Advisory Council. We thank Dan McKenzie and Rob Westaway for many helpful discussions, and a reviewer for useful comments on the manuscript. H. Campbell helped with draughting. This is Cambridge University Earth Sciences Contribution No. 987.

References

Academy of Sciences, Albania, 1983. The earthquake of 1979 April 15 and the elimination of its consequences, *Reports and papers on the Shkodra symposium, 1980*, Nentori Publishing House, Tirana.

Aki, K. & Richards, P. G., 1980. *Quantitative Seismology*, 2 volumes, W. H. Freeman & Co., San Francisco.

Aliaj, S., 1982. Basic seismotectonic features of Albania, in *Earthquake Risk Reduction in the Balkan Region. Working Group A, Seismology, Seismotectonics, Seismic Hazard and Earthquake Prediction*, Final Report, A27–A31.

Ambraseys, N. N., 1966. Seismic environment of the Skopje earthquake of July, 1963, *Rev. de l'Union int. de Secours*, **5**, 1–19.

Ambraseys, N. N., 1975. Studies in historical seismicity and tectonics, in *Geodynamics Today*, pp. 7–16, Royal Society, London.

Ambraseys, N. N. & Melville, C. P., 1982. *A History of Persian Earthquakes*, Cambridge University Press.

Ambraseys, N. N. & Morgenstern, N., 1966. *Field report on the Skopje earthquake of July 26, 1963*, Department of Civil Engineering, Imperial College of Science & Technology, London.

Anderson, H. J., 1985. Seismotectonics of the western Mediterranean, *PhD thesis*, University of Cambridge.

Argand, E., 1924. La tectonique de l'Asie, *Proc. Int. Geol. Congr.*, **XIII**, 171–372.

Arsovski, M., 1970. Contemporary tectonic properties of some seismic active zones in Yugoslavia, *Bulgarian Acad. Sci., Earthquake Engineering, Proc. 3rd Europ. Symp. Earthquake Engineering, Sofia, 1970*, 181–188.

Arsovski, M. & Hadzievski, D., 1970. Correlation between neotectonics and seismicity of Macedonia, *Tectonophys.*, **9**, 129–142.

Arsovski, M., Gojgic, D., Griljic, N., Mitrev, T. & Hadzievski, D., 1966. Summary of the seismo-geologic investigation in the Skopje valley, *Univ. Skopje, Inst. of Seismology, Earthquake Engineering and Town Planning*, **1**.

Barazangi, M. & Dorman, J., 1969. World seismicity map from ESSA, Coast and Geodetic Survey, 1961–1967. *Bull. seism. Soc. Am.*, **59**, 369–380.

Barbano, M. S., Cosentino, M., Lombardo, G. & Patane, G., 1980. Isoseismal maps of Calabria and Sicily earthquakes (southern Italy). *Consiglio nazionale delle richerche progetto finalizzato geodinamica, Publ. no. 341*, Univ. di Catania, Italy.

Berberian, M., Jackson, J. A., Ghorashi, M. & Kadjar, M. H., 1984. Field and teleseismic observations of the 1981 Golbaf-Sirch earthquakes in SE Iran, *Geophys. J. R. astr. Soc.*, **77**, 809–838.

Berg, G. V., 1964. *The Skopje, Yugoslavia, earthquake, July 26, 1963*, American Iron and Steel Institute.

Boore, D. M., Sims, J. D., Kanamori, H. & Harding, S., 1981. The Montenegro, Yugoslavia earthquake of April 15, 1979: source orientation and strength, *Phys. Earth planet. Int.*, **27**, 133–142.

Brooks, M. & Ferentinos, G., 1984. Tectonics and sedimentation in the Gulf of Corinth and the Zakynthos and Kefallinia Channels, western Greece, *Tectonophys.*, **101**, 25–54.

Cagnetti, V. & Pasquale, V., 1979. The earthquake sequence in Friuli, Italy, 1976, *Bull. seism. Soc. Am.*, **69(6)**, 1797–1818.

Calcagnile, G. & Panza, G. F., 1982. The main characteristics of the lithosphere–asthenosphere system in Italy and surrounding regions, *Pure appl. Geophys.*, **119**, 865–879.

Celet, P., 1977. The Dinaric and Aegean arcs: the geology of the Adriatic, in *The Ocean Basins and Margins, 4A*, pp. 215–261, eds Nairn, A. E. M., Kanes, W. H. & Stehli, F. G.

Channell, J. E. T., D'Argenio, B. & Horvath, F., 1979. Adria, the African promontory, in Mesozoic Mediterranean palaeogeography, *Earth Sci. Rev.*, **15**, 213–292.

Chase, C. G., 1978. Plate kinematics: the Americans, East Africa and the rest of the world, *Earth planet Sci. Lett.*, **37**, 355–368.

Christensen, D. H. & Ruff, L. J., 1985. Analysis of the trade-off between hypocentral depth and source time function, *Bull. seism. Soc. Am.*, **75**, 1637–1656.

Cipar, J., 1980. Teleseismic observations of the 1976 Friuli, Italy earthquake sequence, *Bull. seism. Soc. Am.*, **70**, 963–983.

Cipar, J., 1981. Broadband time domain modelling of earthquakes from Friuli, Italy, *Bull. seism. Soc. Am.*, **71**, 1215–1231.

Console, R. & Favali, P., 1981. Study of the Montenegro earthquake sequence (March–July 1979), *Bull. seism. Soc. Am.*, **71**, 1233–1248.

Cosentino, P. & Mulone, A., 1985. The Belice earthquake of January 15, 1968, in *Atlas of isoseismal maps of Italian earthquakes*, ed. Postpischl, D., Consiglio Nazionale delle Richerche, Roma.

Cvijanovic, D. & Prelogovic, E., 1977. Seismicity and neotectonic movements of the Croatian region (SFR Yugoslavia), *Publ. Inst. Geophys. Pol. Acad. Sci.*, **A5(116)**, 281–290.

D'Argenio, B. & Horvath, F., 1984. Some remarks on the deformation history of Adria, from the Mesozoic to the Tertiary, *Ann. Geophys.*, **2(2)**, 143–146.

D'Argenio, B., Horvath, F. & Channell, J. E. T., 1980. Palaeotectonic evolution of Adria, the African promontory, in *Géologie des Chaînes alpines issues de la Tethys*, eds Aubouin, J., Debelmas, J. & Latreille, M., *Mém. Bur. Rech. Géol. Min.*, **115**, 331–351.

de Panfilis, M. & Marcelli, L., 1968. Il periodo sismico della Sicilia occidentale inizato il 14 Gennaio 1968, *Annls. Geofis.*, **XXI**, 343–421.

del Pezzo, E. & Martini, M., 1982. The April 15, 1978 event of the Gulf of Patti, Sicily, and its aftershocks sequence, *Boll. Geof. teor. appl.*, **XXIV(94)**, 109–119.

del Pezzo, E., Maresca, R., Martini, M. & Scarpa, R., 1984. Seismicity of the Aeolian islands, southern Italy, *Ann. Geophys.*, **2(2)**, 173–180.

Deschamps, A. & King, G. C. P., 1983. The Campania–Lucania (southern Italy) earthquake of 23 November, 1980, *Earth planet. Sci. Lett.*, **62**, 296–304.

Deschamps, A. & King, G. C. P., 1984. Aftershocks of the Campania–Lucania (Italy) earthquake of 23 November 1980, *Bull. seism. Soc. Am.*, **74**, 2483–2517.

Deschamps, A., Iannaccone, G. & Scarpa, R., 1984. The Umbrian earthquake (Italy) of 19 September, 1979, *Ann. Geophys.*, **2(1)**, 29–36.

Di Filippo, D. & Peronaci, F., 1962. Contributo alla tectonica delle Alpi Dinariche, *Annls. Geofis.*, **15**, 379–397.

Dragasevic, T., 1973. Savremena grada Zemljine kore i gornjeg omotaca na podrucju Jugoslavije, *Vesnik, Knj.*, **XIV/XV**, Ser. C, 41–52.

Dziewonski, A. M. & Woodhouse, J. H., 1983. Studies of the seismic source using normal-mode theory, in *Earthquakes: Observations Theory and Interpretation*, pp. 45–137, eds, Kanamori, H. & Boschi, E., Italian Physical Society, North Holland Publishing Co., Amsterdam.

Dziewonski, A. M., Chou, T. A. & Woodhouse, J. H., 1981. Determination of earthquake source parameters from waveform data for studies of global and regional seismicity, *J. geophys. Res.*, **86**, 2825–2852.

Dziewonski, A. M., Friedman, A. & Woodhouse, J. H., 1983. Centroid-moment tensor solutions for January–March, 1983, *Phys. Earth planet. Int.*, **33**, 71–75.

Dziewonski, A. M., Franzen, J. E. & Woodhouse, J. H., 1985. Centroid-moment tensor solutions for April–June, 1984, *Phys. Earth planet. Int.*, **37**, 87–96.

Fitch, T. J. & Muirhead, K. J., 1974. Depths to larger earthquakes associated with crustal loading, *Geophys. J. R. astr. Soc.*, **37**, 285–296.

Gasparini, C., Gasperini, M., Iannaccone, G., Napoleone, G., Scarpa, R., Stucchi, M., Taccetti, Q. & Zonno, G., 1980. Seismometrical observations: elaboration and preliminary interpretation of the Norcia earthquake, 1979, *Annls. Geofis.*, **33**, 101–119.

Gasparini, C., Iannaccone, G., Scandone, P. & Scarpa, R., 1982. Seismotectonics of the Calabrian arc, *Tectonophys.*, **84**, 267–286.

Gasparini, C., Iannaccone, G. & Scarpa, R., 1985. Fault-plane solutions and seismicity of the Italian peninsula, *Tectonophys.*, **117**, 59–78.

Ghisetti, F., Scarpa, R. & Vezzani, L., 1982. Seismic activity, deep structures and deformation processes in the Calabrian arc, southern Italy, *Earth Evol. Sci.*, **3**, 248–260.

Giardini, D., Dziewonski, A. M., Woodhouse, J. H. & Boschi, E., 1984. Systematic analysis of the seismicity of the Mediterranean region using the centroid-moment tensor method, *Bull. Geofis. teor. appl.*, **XXVI(103)**, 121–142.

Giese, P. & Reutter, K.-J., 1978. Crustal and structural features of the margins of the Adria microplate, in *Alps, Apennines, Hellenides*, pp. 565–588, eds Closs, H., Roeder, D. & Schmidt, K., Schweizerbart, Stuttgart.

Hsu, K. J., 1982. Alpine Mediterranean geodynamics: past, present and future, in *Alpine Mediterranean Geodynamics*, eds Berckhemer, H. & Hsu, K. J., *Am. Geophys. Un. Geodyn. ser.*, **7**, 7–14.

Hurtig, E. & Neunhofer, H., 1980. *Seismologische expedition des zentralinstituts fur Physik der Erde der AdW in das Herdgebiet des Erdbebens vom 15 April 1979 in Montenegro (SFR Jugoslawien)*, Zentralinstitut Fur Physik der Erde, Potsdam.

I.F.P., 1966. *Etude Géologique de l'Epire (Grece nord-occidentale)*, 2 vols., Paris Editions Technip (L'Institut de Géologie et Recherches du sous-sol, Athenes, et Institut Francais du Petrole).

Irby, W. L., Jacobs, W. S., Minsch, J. H., Needham, R. E., Person, W. J., Presgrave, B. W. & Schmieder, W. H., 1985a. *Preliminary determination of epicenters, September 1984*, Monthly Listing, National Earthquake Information Service, U.S. Department of the Interior, Washington.

Irby, W. L., Jacobs, W. S., Minsch, J. H., Needham, R. H., Person, W. J., Presgrave, B. W. & Schmieder, W. H., 1985b. *Preliminary determination of epicenters, July 1984*, Monthly Listing, National Earthquake Information Service, U.S. Department of the Interior, Washington.

Jackson, J. A., 1979. Active faulting and continental deformation, *PhD thesis*, University of Cambridge.

Jackson, J. A. & Fitch, T. J., 1979. Seismotectonic implications of relocated aftershock sequences in Iran and Turkey, *Geophys. J. R. astr. Soc.*, **57**, 209–229.

Jackson, J. A. & McKenzie, D. P., 1984. Active tectonics of the Alpine–Himalayan belt between western Turkey and Pakistan, *Geophys. J. R. astr. Soc.*, **77**, 185–264.

Jackson, J. A. & McKenzie, D. P., 1988. The relationship between plate motions and seismic moment tensors, and the rates of active deformation in the Mediterranean and Middle East, *Geophys. J. R. astr. Soc.*, in press.

Jackson, J. A., Gagnepain, J., Houseman, G., King, G. C. P., Papadimitriou, P., Soufleris, C. & Virieux, J., 1982a. Seismicity, normal faulting, and the geomorphological development of the Gulf of Corinth (Greece): the Corinth earthquakes of February and March 1981, *Earth planet. Sci. Lett.*, **57**, 377–397.

Jackson, J. A., King, G. & Vita-Finzi, C., 1982b. The neotectonics of the Aegean: an alternative view, *Earth planet. Sci. Lett.*, **61**, 303–318.

Kadinsky-Cade, K. & Barazangi, M., 1982. Seismotectonics of southern Iran: the Oman line, *Tectonics*, **1(5)**, 389–412.

Kanamori, H. & Given, J. W., 1981. Use of long-period surface waves for rapid determination of earthquake-source parameters, *Phys. Earth planet. Int.*, **27**, 8–31.

King, G., Tselentis, A., Gomberg, J., Molnar, P., Roecker, S., Sinvhal, H., Soufleris, C. & Stock, J., 1983. Microearthquake seismicity and active tectonics of northwestern Greece, *Earth planet. Sci. Lett.*, **66**, 279–288.

King, G., Ouyang, Z., Papadimitriou, P., Deschamps, A., Gagnepain, J., Houseman, G., Jackson, J., Soufleris, C. & Virieux, J., 1985. The evolution of the Gulf of Corinth (Greece): an aftershock study of the 1981 earthquakes, *Geophys. J. R. astr. Soc.*, **80**, 677–693.

Kociaj, S. & Sulstarova, E., 1980. The earthquake of June 1, 1905. Shkodra, Albania; intensity distribution and macroseismic epicentre, *Tectonophys.*, **67**, 319–332.

Kostrov, B. V., 1974. Seismic moment and energy of earthquakes, and seismic flow of rock, *Izv. Acad. Sci. USSR Phys. Solid Earth*, **1**, 23–40.

Langston, C. A. & Franco-Spera, M., 1985. Modelling of the Koyna, India, aftershock of 12 December 1967, *Bull. seims. Soc. Am.*, **75(3)**, 651–661.

Langston, C. A. & Helmberger, D. V., 1975. A procedure for modelling shallow dislocation sources, *Geophys. J. R. astr. Soc.*, **42**, 117–130.

Lavecchia, G., Minelli, G. & Pialli, G., 1984. L'appennino umbro-marchigiano: tettonica distensiva e ipotesi di sismogenesi, *Boll. Soc. geol. Ital.*, **103**, 467–476.

Mantovani, E., Babbucci, D. & Farsi, F., 1985. Tertiary evolution of the Mediterranean region: major outstanding problems, *Boll. Geofis. teor. appl.*, **27**, 67–90.

McKenzie, D. P., 1972. Active tectonics of the Mediterranean Region, *Geophys. J. R. astr. Soc.*, **30**, 109–185.

McKenzie, D. P., 1978. Active tectonics of the Alpine–Himalayan belt: the Aegean Sea and surrounding regions, *Geophys. J. R. astr. Soc.*, **55**, 217–254.

McKenzie, D. P. & Jackson, J. A., 1983. The relationship between strain rates, crustal thickening, paleomagnetism, finite strain, and fault movements within a deforming zone, *Earth planet. Sci. Lett.*, **65**, 182–202.

McKenzie, D. P. & Jackson, J. A., 1986. A block model of distributed deformation by faulting, *J. Geol. Soc. London*, **143**, 349–353.

Mercier, J. L., Carey, E., Philip, H. & Sorel, D., 1976. La neotéctonique plio-quaternaire de l'arc egéen externe et de la mer Egee et ses relations avec la seismicite, *Bull. soc. géol. Fr.*, **7(XVIII)**, 355–372.

Mercier, J. L., Delibassis, N., Gauthier, A., Jarrige, J.-J., Lemeille, F., Philip, H., Sebrier, M. & Sorel, D., 1979. La neotectonique de l'arc egeen, *Rev. geol. syn. geogr. phys.*, **21**, 67–92.

Minster, J. B. & Jordan, T. H., 1978. Present day plate motions, *J. geophys. Res.*, **83**, 5331–5334.

Molin, D. & Margottini, C., 1984. Il terremoto del 1627 nella Capitanata Settentrionale, in *Contributo Sismicita del territorio Italiano, Udine, 12 May 1981*, pp. 251–279, Publs. Commissione ENEA-ENEL.

Molnar, P. & Tapponnier, P., 1981. A possible dependence of tectonic strength on the age of the crust in Asia, *Earth planet. Sci. Lett.*, **52**, 107–114.

Morelli, C., 1984. Promontorio Africano o microplacca Adriatica, *Boll. Ocean. teor. appl.*, **II(2)**, 151–168.

Morelli, C., Giese, P., Cassinis, R., Colombi, B., Guerra, I., Luongo, G., Scarascia, S. & Schutte, K.-G., 1975. Crustal structure of southern Italy. A seismic refraction profile between Puglia–Calabria–Sicily, *Boll. Geofis. teor. appl.*, **XVII(67)**, 183–210.

Mulargia, F. & Boschi, E., 1982. The 1908 Messina earthquake and related seismicity, in *Earthquakes: observation, theory and interpretation*, pp. 493–518, eds Kanamori, H. & Boschi, E., Italian Physical Society, North Holland Publishing Co, Amsterdam.

Nicholich, R., 1981. Crustal structures in the Italian peninsula and surrounding seas: a review of DSS data, in *Sedimentary Basins of Mediterranean Margins*, pp. 3–17, ed. Wezel, F. C., C.N.R. Italian Project of Oceanography, Italy.

Ouyed, M., Yielding, G., Hatzfeld, D. & King, G. C. P., 1983. An aftershock study of the El Asnam (Algeria) earthquake of 1980 October 10, *Geophys. J. R. astr. Soc.*, **73**, 605–639.

Papazachos, B. C., 1973. Distribution of seismic foci in the Mediterranean and surrounding area and its tectonic implication, *Geophys. J. R. astr. Soc.*, **33**, 421–430.

Philip, H., 1983. La tectonique actuelle et recente dans le domaine mediterraneen et ses bordures, ses relations avec la sismicite, *These*, Univ. des Sc. K.-G.-ch. du Languedoc. Montpellier.

Ritsema, A. R., 1975. The contribution of the study of seismicity and earthquake mechanisms to the knowledge of Mediterranean geodynamic processes, in *Progress in Geodynamics*, pp. 142–153, Amsterdam.

Ryan, W. B. F. & Heezen, B. C., 1965. Ionian sea submarine canyons and the 1908 Messina turbidity current, *Bull. geol. Soc. Am.*, **76**, 915–932.

Schick, R., 1977. Eine seismotektonische Bearbeitung des Erdbebens von Messina im Jahre 1908, *Geol. Jb.*, **E-11**, 3–74.

Scott, D. R. & Kanamori, H., 1985. On the consistency of moment tensor source mechanisms with first-motion data, *Phys. Earth planet. Int.*, **37**, 97–107.

Sorsky, A. A., 1968. Geological and tectonic factors in the Skopje earthquake of 26 July 1963, in *The Skopje earthquake of 26 July 1963*, Report of the Unesco Technical Assistance Mission, Unesco.

Soufleris, C., 1980. The Thessaloniki (north Greece) 1978 earthquake sequence, *PhD thesis*, University of Cambridge.

Soufleris, C. & Stewart, G., 1981. A source study of the Thessaloniki (northern Greece) 1978 earthquake sequence, *Geophys. J. R. astr. Soc.*, **67**, 343–358.

Soufleris, C., Jackson, J., King, G., Spencer, C. & Scholz, C., 1982. The 1978 earthquake sequence near Thessaloniki (northern Greece), *Geophys. J. R. astr. Soc.*, **68**, 429–458.

Stein, S., Wiens, D. A. & Fujita, K., 1982. The 1966 Kremasta reservoir earthquake sequence, *Earth planet. Sci. Lett.*, **59**, 49–60.

Suess, E., 1883. *Das Antlitz der Erde*, Tempsky (Prague) und Freytag (Leipzig).

Sulstarova, E., 1980. Some characteristics of earthquake foci in Albania and the field of tectonic stress, *Publ. Inst. Geophys. Pol. Acad. Sci.*, **A-9(135)**, 79–86.

Sulstarova, E., 1982. The focal mechanisms of earthquakes in Albania, in *Earthquake Risk Reduction in the Balkan region, Working Group A, Seismology, Seismotectonics, Seismic Hazards and Earthquake Predictions*, Final Report, A32-A38.

Sulstarova, E. & Kociaj, S., 1980. The Dibra (Albania) earthquake of November 30, 1967, *Tectonophys.*, **67**, 333–343.

Sulstarova, E., Kociaj, S. & Aliaj, S., 1982. Seismic focal zones in Albania, indicated by seismological and geological data, in *Earthquake Risk Reduction in the Balkan region. Working Group A, Seismology, Seismotectonics, Seismic Hazards and Earthquake Predictions*, Final Report, A22-A25.

Vandenberg, J., 1983. Reappraisal of paleomagnetic data from Gargano (South Italy), *Tectonophys.*, **98**, 29–41.

Vandenberg, J. & Zijderveld, J. D. A., 1982. Paleomagnetism in the Mediterranean area, in *Alpine Mediterranean Geodynamics*, eds Berckhemer, H. & Hsu, K. J., *Am. Geophys. Un. Geodyn. ser.*, **7**, 83–112.

Walcott, R. I., 1984. The kinematics of the plate boundary zone through New Zealand: a comparison of short- and long-term deformations, *Geophys. J. R. astr. Soc.*, **79**, 613–633.

Weber, C. & Courtot, P., 1978. Le seisme du Frioul (Italie, 6 mai 1976) dans son contexte sismotectonique, *Rev. Géogr. phys. Géol. dyn.*, **2(XX)**, 247–258.

Westaway, R., 1987. The Campania, Southern Italy, earthquakes of 21 August 1962, *Geophys. J. R. astr. Soc.*, **88**, 1–24.

Westaway, R. W. C. & Jackson, J. A., 1984. Surface faulting in the southern Italian Campania–Basilicata earthquake of 23 November 1980, *Nature*, **312(5993)**, 436–438.

Westaway, R. & Jackson, J., 1987. The earthquake of 23 November 1980 in Campania–Basilicata (S. Italy), *Geophys. J. R. astr. Soc.*, **90**, 375–443.

Yielding, G., Jackson, J. A., King, G. C. P., Sinvhal, H., Vita-Finzi, C. & Wood, R. M., 1981. Relations between surface deformation, fault geometry, seismicity and rupture characteristics during the El Asnam (Algeria) earthquake of 10 October 1980, *Earth planet. Sci. Lett.*, **56**, 287–304.

Zatopek, A., 1968. The Skopje earthquake of 26 July 1963 and the seismicity of Macedonia, in *The Skopje earthquake of 26 July 1963*, Report of the Unesco Technical Assistance Mission, Unesco.

Zonno, G. & Kind, R., 1984. Depth determination of North Italian earthquakes using Grafenberg data, *Bull. seism. Soc. Am.*, **74(5)**, 1645–1659.

Appendix 1

Location information for focal mechanisms figures in this study. Latitude, longitude and depth are derived mainly from USGS listings but some information is based on relative relocations, macroseismic and waveform modelling studies. All other data, such as magnitudes, origin time and number of stations reporting the event were determined from USGS data.

NO.	DATE	LAT	LONG	DEPTH	m_b	STNS	HR	MIN	SEC	M_s
1.	081228	38.10	15.35	10.	7.0	0	4	20	00.0	-
2	530812	38.11	20.72	0.	7.2	0	9	25	51.2	-
3	591115	37.80	20.56	0.	6.6	0	17	8	40.5	-
4	620111	43.30	17.35	10.	5.7	0	5	5	4.1	-
5	620821	41.02	14.98	8.	-	27	18	19	35.3	-
6	630726	42.100	21.400	5.	5.5	222	4	17	12.5	-
7	631216	37.100	20.900	15.	5.6	45	13	47	56.4	-
8	640415	45.300	18.100	33.	5.4	51	8	30	3.6	-
9	660205	39.02	21.82	8.	5.6	109	02	01	45.5	-
10	661029	38.81	21.10	20.	5.7	50	02	39	29.4	-
11	670501	39.430	21.190	11.	5.6	88	7	9	0.5	-
12	671130	41.41	20.44	21.	6.0	92	7	25	51.5	-
13	680115	37.750	12.983	10.	5.4	65	2	1	8.5	-
14	680116	37.857	12.976	36.	5.1	71	16	42	44.3	-
15	680125	37.687	12.966	3.	5.1	69	9	56	48.7	-
16	680328	37.900	20.900	6.	5.4	94	7	39	57.1	-
17	690403	40.500	19.900	18.	5.1	86	22	12	25.8	5.5
18	690708	37.561	20.277	33.	5.4	97	8	9	17.5	5.4
19	691013	39.570	20.630	8.	5.6	106	1	2	28.5	5.0
20	691026	44.874	17.286	33.	5.5	81	15	36	51.8	5.6
21	691027	44.923	17.232	33.	5.3	117	8	10	58.3	6.1
22	700819	41.099	19.771	33.	5.2	101	2	1	53.1	5.7
23	710715	44.776	10.335	8.	5.2	99	1	35	22.3	-
24	720917	38.283	20.340	33.	5.6	114	14	7	15.6	6.3
25	731104	38.896	20.441	8.	5.8	99	15	52	11.7	5.5
26	760506	46.356	13.275	9.	6.0	275	20	0	11.6	6.5
27	760511	37.560	20.352	33.	5.8	202	16	59	48.2	6.4
28	760612	37.545	20.551	8.	5.5	160	0	59	16.9	5.3
29	760911	46.280	13.157	16.	5.2	120	16	31	12.0	5.5
30	760911	46.299	13.203	20.	5.3	114	16	35	3.3	5.4
31	760915	46.302	13.197	10.	5.7	257	3	15	19.9	6.0
32	760915	46.322	13.132	17.	5.4	240	9	21	19.1	5.9
33	780415	38.391	15.066	21.	5.5	241	23	33	47.2	5.7

Appendix 1—*continued*

NO.	DATE	LAT	LONG	DEPTH	m_b	STNS	HR	MIN	SEC	M_s
34	790409	41.956	19.023	10.	5.3	196	2	10	20.3	4.9
35	790415	42.096	19.209	10.	6.2	217	6	19	44.1	6.9
36	790415	42.319	18.682	10.	5.7	291	14	43	6.0	5.6
37	790524	42.255	18.752	8.	5.8	342	17	23	18.2	6.2
38	790919	42.812	13.061	16.	5.9	175	21	35	37.2	5.8
39	791208	38.284	11.741	33.	5.4	190	4	6	34.3	5.3
40	800518	43.294	20.837	9.	5.7	164	20	2	57.5	5.8
41	800528	38.482	14.252	12.	5.7	232	19	51	19.3	5.5
42	801123	40.760	15.330	10.	6.0	265	18	34	53.8	6.9
43	810813	44.849	17.312	16.	5.4	143	2	58	11.9	5.5
44	821116	40.883	19.590	21.	5.6	241	23	41	21.0	5.5
45	830117	38.026	20.228	14.	6.1	329	12	41	29.7	7.0
46	830323	38.294	20.262	19.	5.8	258	23	51	6.5	6.2
47	840429	43.260	12.558	12.	5.2	202	5	3	0.0	5.3
48	840507	41.765	13.898	10.	5.5	302	17	49	41.6	5.8
49	840511	41.831	13.961	14.	5.2	259	10	41	49.9	5.2
50	840513	42.967	17.734	30.	5.1	190	12	45	55.8	5.1
51	840709	40.677	21.831	10.	5.1	208	18	57	09.6	4.9

Appendix 2

Strike, dip and rake of events described in Appendix 1. Convention follows Aki & Richards (1980). Rake was determined graphically.

	NODAL PLANE 1			NODAL PLANE 2		
EVENT NO.	STRIKE	DIP	RAKE	STRIKE	DIP	RAKE
1	208	55		349	42	
2	163	34		330	56	
3	310	83		066	16	
4	197	80	149	293	60	12
5	310	65	-110	171	32	-54
6	303	74	-21	039	70	-163
7	064	64	90	244	26	90
8	302	55	100	104	36	76
9	252	66	-100	096	26	-69
10	204	70	113	334	30	43
11	197	56	-44	315	56	-137
12	200	58	-80	0	34	-106
13	270	50	35	156	64	134
14	250	58	18	150	75	147
15	270	64	31	165	62	150
16	120	71	65	357	31	141
17	164	40	97	336	50	84
18	145	88	90	325	02	90
19	092	83	61	352	30	166
20	228	88	12	138	78	178
21	066	90	0	336	90	180
22	152	71	90	332	19	90
23	250	84	132	346	42	9
24	306	80	-26	042	65	-168
25	336	44	90	156	46	90
26	076	75	87	267	15	101
27	172	80	90	352	10	90
28	115	70	90	295	20	90
29	076	73	90	256	17	90
30	091	80	90	271	10	90
31	270	40	126	047	59	64
32	061	68	61	297	36	140
33	148	55	153	254	68	38
34	180	80	101	312	15	43

Appendix 2–*continued*

EVENT NO.	NODAL PLANE 1			NODAL PLANE 2		
	STRIKE	DIP	RAKE	STRIKE	DIP	RAKE
35	121	72	88	307	18	96
36	148	90	91	238	1	0
37	154	70	90	334	20	90
38	320	66	-141	212	55	-30
39	254	56	136	012	55	43
40	294	83	0	204	90	173
41	052	62	64	278	37	130
42	317	62	-80	116	30	-108
43	165	60	-172	071	83	-30
44	297	35	54	159	63	112
45	135	83	90	315	7	90
46	027	59	175	120	86	32
47	143	21	-72	304	70	-97
48	174	31	-52	312	66	-110
49	156	43	-76	317	49	-103
50	311	16	112	108	75	84
51	212	38	-105	051	54	-79